

# NATIONAL ADVISORY COMMITTEE FOR AERONAUTICS

## TECHNICAL NOTE

No. 1876

### CALCULATION OF THE AERODYNAMIC LOADING OF FLEXIBLE WINGS OF ARBITRARY PLAN FORM AND STIFFNESS

By Franklin W. Diederich

Langley Aeronautical Laboratory  
Langley Air Force Base, Va.

**DISTRIBUTION STATEMENT A**  
Approved for Public Release  
Distribution Unlimited

20000803 206



Washington  
April 1949

**Reproduced From  
Best Available Copy**

**DTIC QUALITY INSPECTED 4**

AQM00-10-3141

— *Capt. Cropper*

ERRATA

NACA TN 1876

CALCULATION OF THE AERODYNAMIC LOADING OF FLEXIBLE WINGS  
OF ARBITRARY PLAN FORM AND STIFFNESS

By Franklin W. Diederich

April 1949

Equations (32), (32a), (35a), and (36a) on pages 18 and 19 are in error  
in that a  $\cos \Lambda$  factor has been omitted. The correct expressions are:

$$cc_l = cm_{e1} \left( \frac{m_e}{m_{e1}} \bar{\alpha} \right) \cos \Lambda \quad (32)$$

$$\frac{cc_l}{c_r} = m_{e1} \frac{c}{c_r} \left( \frac{m_e}{m_{e1}} \bar{\alpha} \right) \cos \Lambda \quad (32a)$$

$$C_{L_w} = m_{e1} \cos \Lambda \frac{s_w c_r}{S/2} [K_1]_1 \begin{bmatrix} \frac{c}{c_r} \end{bmatrix}^o \left\{ \frac{m_e}{m_{e1}} \bar{\alpha} \right\} \quad (35a)$$

$$C_{BM_w} = m_{e1} \cos \Lambda \frac{s_w c_r}{S/2} \frac{s_w}{2b} [K_2]_1 \begin{bmatrix} \frac{c}{c_r} \end{bmatrix}^o \left\{ \frac{m_e}{m_{e1}} \bar{\alpha} \right\} \quad (36a)$$

NATIONAL ADVISORY COMMITTEE FOR AERONAUTICS

TECHNICAL NOTE NO. 1876

CALCULATION OF THE AERODYNAMIC LOADING OF FLEXIBLE WINGS  
OF ARBITRARY PLAN FORM AND STIFFNESS

By Franklin W. Diederich

SUMMARY

A method is presented for calculating the aerodynamic loading, the divergence speed, and certain stability derivatives of wings and tail surfaces of arbitrary plan form and stiffness. Provision is made for using either stiffness curves and root-rotation constants or influence coefficients in the analysis. Computing forms, tables of numerical constants required in the analysis, and an illustrative example are included to facilitate calculations by means of the method.

INTRODUCTION

The distribution of the aerodynamic loading on wings and tail surfaces is important both for the structural analysis of these components, since it determines the applied bending moment and torque acting at any station, and for their aerodynamic analysis, since it affects the stability derivatives to a large extent. At high speeds the aerodynamic loading, particularly in the case of swept wings, is greatly affected by the structural deformations caused by the loading. The present paper is concerned with the determination of the effects of structural flexibility on the aerodynamic loading of wings of arbitrary plan form and stiffness.

The problem of load distribution was analyzed for unswept flexible wings as early as 1926 (reference 1) but has received relatively little attention since that time. The only new effect considered in subsequent work is aerodynamic induction (reference 2). No work appears to have been done on the loading of flexible swept wings. The related problem of aeroelastic divergence of swept wings with certain prescribed stiffness variations has been treated in reference 3.

The present paper treats the problem of aerodynamic loading by matrix methods. Aerodynamic induction is taken into account approximately, since suitable aerodynamic influence coefficients are not available for wings of arbitrary plan form. When they become available they can readily be incorporated in this method. Structural flexibility is taken into account in the form of either calculated stiffness variations or measured influence coefficients. The required integrating matrices

are presented for both a six-point and a ten-point solution. For the six-point solution convenient computing forms are included as well. The method is illustrated by means of an example. In addition to the analysis of the aerodynamic loading, the determination of the related divergence speed and of certain stability derivatives is discussed.

For the convenience of the reader unfamiliar with matrix terminology a summary of matrix methods has been included in the appendix. The sections on "Application of the Method" and, in particular, "Instructions for Solution" may be read without reference to the section "Derivation of the Method."

### SYMBOLS

A	aspect ratio $\left(\frac{b^2}{S}\right)$
[A]	aeroelastic matrix
a	dimensionless parameter $\left(\frac{m_e q S \Lambda^2 e_{l_r} c_r^2 \cos^4 \Lambda}{(GJ)_r}\right)$
a'	parameter $(m_e q S_w c_r \cos \Lambda)$
ac	section aerodynamic center, measured from leading edge, fraction of chord
b	wing span, inches
c	chord measured parallel to the air stream, inches
$\bar{c}$	average wing chord, inches $\left(\frac{S}{b}\right)$
$c_l$	section lift coefficient $\left(\frac{l'}{qc}\right)$
$C_{l_w}$	wing lift coefficient $\left(\frac{L_w}{qS}\right)$
$C_{BM_w}$	wing root bending-moment coefficient $\left(\frac{M'_r}{qSb}\right)$
$C_{l_w}$	wing rolling-moment coefficient $(2C_{BM_w})$

- d dimensionless parameter  $\left( \frac{m_e q s \Lambda^3 c_r \tan \Lambda \cos^3 \Lambda}{(EI)_r} \right)$
- EI bending stiffness in planes perpendicular to the elastic axis, pound-inches<sup>2</sup>
- e location of elastic axis measured from leading edge, fraction of chord
- e<sub>1</sub> distance from reference axis to section aerodynamic center (positive forward), fraction of chord
- GJ torsional stiffness in planes perpendicular to the elastic axis, pound-inches<sup>2</sup>
- [I] unit matrix
- [I<sub>0</sub>] matrix defined by equation (12)
- [K<sub>1</sub>] integrating matrix for single integration from tip to root
- [K<sub>1</sub>]<sub>1</sub> first row of K<sub>1</sub> matrix
- [K<sub>2</sub>] integrating matrix for double integration from tip to root
- [K<sub>2</sub>]<sub>1</sub> first row of K<sub>2</sub> matrix
- [K<sub>3</sub>] integrating matrix for single integration from root to tip
- [K<sub>4</sub>] matrix relating concentrated and accumulated torque
- [K<sub>5</sub>] matrix relating concentrated loads and accumulated bending moments
- [K<sub>6</sub>] matrix converting torques due to distributed loads to torques due to concentrated torques
- [K<sub>7</sub>] matrix converting bending moments due to distributed loads to bending moments due to concentrated loads
- L<sub>w</sub> lift on both wings but excluding lift on part of wing covered by fuselage, pounds
- l running air load along the reference axis, pounds per inch
- M accumulated bending moment (in planes perpendicular to the reference axis unless specified otherwise), inch-pounds
- m<sub>e</sub> effective section lift-curve slope for angles of attack due to deformation, per radian

$m_{e1}$	effective section lift-curve slope for additional-type angle-of-attack distributions, per radian
$m_o$	section lift-curve slope, per radian
$P$	concentrated load, pounds
$\frac{pb}{2V}$	wing-tip helix angle
$Q_\alpha, Q_\varphi$	root-twist constants (see equation (9))
$Q_T$	root-bending constant (see equation (9))
$q$	dynamic pressure, pounds per square inch
$R$	concentrated torque, inch-pounds
$S$	total wing area including part of wing covered by fuselage, square inches
$s_w$	distance from wing root to wing tip perpendicular to the air stream (see fig. 1), inches
$s_\Lambda$	length of wing along reference axis (see fig. 1), inches
$T$	accumulated torque (in planes perpendicular to the reference axis unless specified otherwise), inch-pounds
$w$	distance between the effective root and the innermost complete section of the torsion box perpendicular to the elastic axis, inches
$y$	lateral ordinate measured from wing root, inches
$\bar{y}$	lateral center of pressure, inches
$\alpha$	angle of attack, radians
$\bar{\alpha}$	equivalent angle of attack, radians $\left( \alpha_s + \frac{m_{e1}}{m_e} \alpha_g \right)$
$\Gamma$	local dihedral angle due to deformation or slope of wing deflection curve at reference axis, radians
$\zeta$	structural deflection, inches
$\eta$	distance along reference axis, inches
$\Lambda$	angle of sweepback (measured to the reference axis unless specified otherwise), degrees

$[\Phi_P]$  influence-coefficient matrix for wing twist in planes parallel to the air stream due to concentrated unit loads applied at the reference axis, radians per pound

$[\Phi_R]$  influence-coefficient matrix for wing twist in planes parallel to the air stream due to concentrated unit torques applied in planes parallel to the air stream, radians per inch-pound

$\phi$  angle of twist in planes perpendicular to the reference axis, radians

Subscripts:

a	additional
c	midchord
D	divergence
fw	flexible wing
g	geometric
LE	leading edge
M	due to bending moment
MAC	pertaining to the mean aerodynamic chord
p	damping in roll
r	at root or effective root
rw	rigid wing
s	structural (due to structural deformations)
sub	subsonic
spr	supersonic
T	due to torque
TE	trailing edge
w	wing exclusive of fuselage

Prime mark:

in or pertaining to sections parallel to air stream rather than perpendicular to the reference axis

Matrix notation:

$\{ \}$	column matrix
$[ ]$	row matrix

$\begin{bmatrix} \end{bmatrix}$  square matrix  
 $\begin{bmatrix} 0 \\ \end{bmatrix}$  diagonal matrix

# DERIVATION OF THE METHOD

## Method Employing Stiffness Curves

Assumptions.— In the development of the method the following assumptions are made:

(a) The effects of aerodynamic induction may be taken into account by applying an over-all correction to strip theory and rounding off the resulting load distribution at the tip.

(b) All deflections and angles of attack are small.

(c) The wing is mounted flexibly at an effective root perpendicular to the elastic axis through the intersection of the elastic axis and the fuselage (see fig. 1), the root rotations being proportional to the root bending moment and root torque.

(d) An elastic axis exists in the outer portion of the wing, this axis being defined as the elastic axis the wing would have if it were mounted rigidly some distance outboard of the root approximately perpendicular to the midchord line. (Near the root the elastic axis is defined as the extension of the outboard elastic axis.)

(e) All deformations are given by the elementary theories of bending and of torsion about the reference axis, which in this case is the elastic axis.

Air loads.— In keeping with assumptions (a) and (b) the force on a wing section of unit width parallel to the direction of flight is

$$\begin{aligned} l' &= qc \left( m_e \alpha_s + m_{e1} \alpha_g \right) \cos \Lambda \\ &= m_e qc \bar{\alpha} \cos \Lambda \end{aligned} \quad (1)$$

where the equivalent angle of attack  $\bar{\alpha}$  is defined by

$$\bar{\alpha} = \alpha_s + \frac{m_{e1}}{m_e} \alpha_g \quad (1a)$$



The effective section lift-curve slope  $m_e$  for angle-of-attack distributions due to structural deformations has been given in reference 3 on the basis of the reasoning of reference 4 for subsonic speeds as

$$m_e = m_0 \frac{A}{A + 4 \cos \Lambda} \quad (2)$$

Similarly, the effective lift-curve slope  $m_{e1}$  for additional-type angle-of-attack distributions is determined by the same reasoning as

$$m_{e1} = m_0 \frac{A}{A + 2 \cos \Lambda} \quad (3)$$

Both slopes must be multiplied by  $\cos \Lambda$ , as in equation (1), in order to apply to loads acting on sections and angles of attack measured in planes parallel to the direction of flight.

The torque of the running load  $l$  about the reference axis is  $l'_{e1c}$  for uncambered sections (for cambered sections the torque at zero lift must be added and the analysis of the following paragraphs modified accordingly). This torque may be resolved into a running torque about the elastic axis and a running bending moment about a line perpendicular to the elastic axis. The running load, torque, and moment must then be multiplied by  $\cos \Lambda$  to yield their values per unit length along the elastic axis, so that

$$l = m_e q c \bar{\alpha} \cos^2 \Lambda \quad (4)$$

or, in matrix notation,

$$\{l\} = m_e q (\cos^2 \Lambda) \begin{bmatrix} 0 \\ c \end{bmatrix} \{\bar{\alpha}\} \quad (4a)$$

The running torque and the running bending moment are, respectively,  $\{l_{e1c} \cos \Lambda\}$  and  $\{-l_{e1c} \sin \Lambda\}$ . The running bending moment leads to accumulated bending moments which have to be added to the accumulated bending moment due to the running load.

The accumulated torque  $T$  is obtained from the running torque by an integration inboard from the tip. This integration may be performed by a matrix  $[K_1]$  which is based on Simpson's rule with a modification suggested by V. M. Falkner at the tip. (See appendix.) The effect of Falkner's modification is to round off the calculated load distribution and cause it to go to zero with an infinite slope at the tip, as the aerodynamic lift distributions actually do. The matrix is given in table I.

Similarly, the accumulated bending moment  $M$  is obtained by a double integration inboard from the tip of the running load and a single integration of the running moment. The double integration may be performed by another matrix  $[K_2]$  (given in table II), which is based on the equivalent of Simpson's rule for moments, Falkner's modification again being made at the tip. The derivation of the integrating matrices is discussed in somewhat greater detail in the appendix.

The accumulated torque and bending moment may then be written as

$$\begin{aligned} \{T\} &= s_\Lambda [K_1] \{l e_{1c} \cos \Lambda\} \\ &= m_e q s_\Lambda e_{1r} c_r^2 (\cos^3 \Lambda) [K_1] \left[ \frac{e_{1r}}{e_{1r}} \left( \frac{c}{c_r} \right)^2 \right] \{\bar{\alpha}\} \end{aligned} \quad (5)$$

and

$$\begin{aligned} \{M\} &= s_\Lambda^2 [K_2] \{l\} - s_\Lambda [K_1] \{l e_{1c} \sin \Lambda\} \\ &= m_e q s_\Lambda^2 c_r (\cos^2 \Lambda) \left[ [K_2] \left[ \frac{c}{c_r} \right] - (\sin \Lambda) \frac{e_{1r} c_r}{s_\Lambda} [K_1] \left[ \frac{e_{1r}}{e_{1r}} \left( \frac{c}{c_r} \right)^2 \right] \right] \{\bar{\alpha}\} \end{aligned} \quad (6)$$

Equations of equilibrium.— The equations of equilibrium of a deformed wing referred to the elastic axis are

$$GJ \frac{d\phi}{dy} = T \quad (7)$$

$$EI \frac{d\Gamma}{dy} = M \quad (8)$$

These equations must be integrated outboard from the root to obtain  $\phi$  and  $\Gamma$ . The integrations may be performed by a matrix  $[K_3]$  (see table III and appendix), also based on Simpson's rule without the tip modification, however, since the torques and moments go to zero with finite and zero slopes, respectively. To the deformations obtained in this manner the rotations due to the root deflection,  $\phi_r$  and  $\Gamma_r$ ,

must be added. The root rotations are defined by four dimensionless constants:

$$Q_{\phi T} = \frac{\phi_{rT}/T_r}{w/(GJ)_r} \quad (9a)$$

$$Q_{\phi M} = \frac{\phi_{rM}/M_r}{w/(GJ)_r} \quad (9b)$$

$$Q_{\Gamma T} = \frac{\Gamma_{rT}/T_r}{w/(EI)_r} \quad (9c)$$

$$Q_{\Gamma M} = \frac{\Gamma_{rM}/M_r}{w/(EI)_r} \quad (9d)$$

which may be combined into two other constants

$$Q_{\alpha T} = \frac{\alpha_{rT}/T_r}{w/(GJ)_r} = \left( Q_{\phi T} - \frac{(GJ)_r}{(EI)_r} \tan \Lambda Q_{\Gamma T} \right) \cos \Lambda \quad (9e)$$

$$Q_{\alpha M} = \frac{\alpha_{rM}/M_r}{w/(GJ)_r} = \left( Q_{\phi M} - \frac{(GJ)_r}{(EI)_r} \tan \Lambda Q_{\Gamma M} \right) \cos \Lambda \quad (9f)$$

w being defined as in figure 1. The deformations may then be written as

$$\{\phi\} = \frac{s_{\Lambda}}{(GJ)_r} \left[ \left[ K_3 \right] \left[ \frac{(GJ)_r}{GJ} \right] + \frac{w}{s_{\Lambda}} Q_{\phi T} [I_0] \right] \{T\} + \frac{w}{s_{\Lambda}} Q_{\phi M} [I_0] \{M\} \quad (10)$$

and

$$\{\Gamma\} = \frac{s_\Lambda}{(EI)_r} \left[ \left[ K_3 \right] \left[ \frac{\overset{\circ}{(EI)}_r}{EI} \right] + \frac{w}{s_\Lambda} Q_{TM} [I_O] \right] \{M\} + \frac{w}{s_\Lambda} Q_{TT} [I_O] \{T\} \quad (11)$$

where the matrix  $[I_O]$  is defined by

$$[I_O] = \begin{bmatrix} 0 & 0 & 0 & 0 & 0 & \dots \\ 1 & 0 & 0 & 0 & 0 & \dots \\ 1 & 0 & 0 & 0 & 0 & \dots \\ 1 & 0 & 0 & 0 & 0 & \dots \\ 1 & 0 & 0 & 0 & 0 & \dots \\ \vdots & \vdots & \vdots & \vdots & \vdots & \ddots \end{bmatrix} \quad (12)$$

The angle of attack due to the structural deformations  $\alpha_s$  is related to  $\varphi$  and  $\Gamma$  by

$$\alpha_s = (\varphi - \Gamma \tan \Lambda) \cos \Lambda \quad (13)$$

If equations (5), (6), (10), and (11) are substituted in the matrix equivalent of equation (13), the following relation is obtained:

$$\{\alpha_s\} = a [A] \{\bar{\alpha}\} \quad (14)$$

where the aeroelastic matrix  $[A]$  is defined by

$$\begin{aligned} [A] = & \left[ [K_3] \left[ \frac{\overset{\circ}{(GJ)}_r}{GJ} \right] + \frac{w}{s_w} (Q_{\omega T} - Q_{\alpha M} \tan \Lambda) [I_O] \right. \\ & \left. + \frac{(GJ)_r}{(EI)_r} (\tan^2 \Lambda) [K_3] \left[ \frac{\overset{\circ}{(EI)}_r}{EI} \right] [K_1] \left[ \frac{\overset{\circ}{e_1}}{e_{1r}} \left( \frac{c}{c_r} \right)^2 \right] \right. \\ & \left. - \left[ \frac{d}{a} [K_3] \left[ \frac{\overset{\circ}{(EI)}_r}{EI} \right] - \frac{w}{s_w} \frac{s_\Lambda}{e_{1r} c_r \cos \Lambda} Q_{\alpha M} [I_O] \right] [K_2] \left[ \frac{\overset{\circ}{c}}{c_r} \right] \right] \end{aligned} \quad (15)$$

and the parameters

$$a = \frac{m_e q s \Lambda^2 e_{1r} c_r^2 \cos^4 \Lambda}{(GJ)_r} \quad (16)$$

and

$$\frac{d}{a} = \frac{(GJ)_r}{(EI)_r} \frac{s \Lambda}{e_{1r} c_r \cos \Lambda} \tan \Lambda \quad (16a)$$

are substantially the same parameters as those used in reference 3.

Solution of the equations.— If it is desired to calculate the aerodynamic loading corresponding to a given geometrical angle-of-attack distribution and dynamic pressure, equation (14) may be rewritten as follows:

$$\left[ [I] - a [A] \begin{Bmatrix} m_e \\ m_{e1} \end{Bmatrix} \bar{\alpha} \right] = \{ \alpha_g \} \quad (17)$$

In this form it constitutes a set of linear simultaneous equations for the  $\bar{\alpha}$  values in terms of  $\alpha_g$  values. From the calculated  $\bar{\alpha}$  values the lift distribution may be determined from either equation (1) or (4).

The divergence dynamic pressure may be obtained from equation (17) by setting the determinant of the square matrix on the left side of the equation equal to zero. This procedure is equivalent to setting  $\alpha_g$  equal to zero in the term  $\bar{\alpha}$  of equation (14), so that

$$\{ \alpha_g \} = a [A] \{ \alpha_g \} \quad (18)$$

The critical value of  $a$  is then determined by matrix iteration and hence the divergence dynamic pressure from equation (16).

#### Method Employing Influence Coefficients

The assumptions made in the preceding sections concerning the behavior of the wing structure are unnecessary if influence coefficients for the given structure are available from test data or refined methods of calculation. The coefficients most convenient for this analysis are those giving the rotation of the structure in planes parallel to the direction of flight due to vertical loads applied along a convenient reference axis and due to torques about lines perpendicular to the

direction of flight. Since it is usually more convenient to apply concentrated rather than distributed loads in structural tests, the influence coefficients are considered in this analysis to have been obtained in this manner.

The angle of structural deformation  $\alpha_s$  may be expressed in terms of the influence coefficients  $\phi_R$  and  $\phi_P$  as follows:

$$\{\alpha_s\} = [\phi_R]\{R\} + [\phi_P]\{P\} \quad (19)$$

where the  $R$ 's and  $P$ 's are arbitrary concentrated torques and loads, the latter being applied at the reference axis. The accumulated torques and bending moments about lines perpendicular and parallel, respectively, to the direction of flight may be related to the concentrated torques and loads by means of the summation matrices  $[K_4]$  and  $[K_5]$  (see appendix) as follows:

$$\{T^s\} = [K_4]\{R\} - \tan \Lambda \{M^s\} \quad (20)$$

$$\{M^s\} = s_w [K_5]\{P\} \quad (21)$$

These relations may be solved for the values of  $R$  and  $P$  required to produce given distributions of accumulated torque and bending moment

$$\{R\} = [K_4]^{-1} \left\{ \{T^s\} + \tan \Lambda \{M^s\} \right\} \quad (22)$$

$$\{P\} = \frac{1}{s_w} [K_5]^{-1} \{M^s\} \quad (23)$$

The accumulated torques and bending moments produced by the air load are then

$$\{T^s\} = s_w [K_1] \{l^s e_{1c}\} - \{M^s\} \tan \Lambda \quad (24)$$

$$\{M^s\} = s_w^2 [K_2] \{l^s\} \quad (25)$$

Upon substituting equations (22), (23), (24), (25), and (1) into equation (19), the following equation is obtained:

$$\{\alpha_B\} = a' [A'] \{\bar{\alpha}\} \quad (26)$$

where

$$a' = m_{eqs} c_r \cos \Lambda \quad (27)$$

and

$$[A'] = \left[ e_{1r} c_r [\Phi_R] [K_6] \left[ \frac{e_1}{e_{1r}} \left( \frac{c}{c_r} \right)^2 \right] + [\Phi_P] [K_7] \left[ \frac{c}{c_r} \right] \right] \quad (28)$$

where, in turn

$$[K_6] = [K_4]^{-1} [K_1] \quad (29a)$$

$$[K_7] = [K_5]^{-1} [K_2] \quad (29b)$$

are given in tables IV and V.

The solution of equation (26) is obtained in the manner previously described for equation (14).

#### APPLICATION OF THE METHOD

##### Determination of the Structural Parameters

At the time an aeroelastic analysis is performed no experimental stiffness data are usually available, so that the calculated stiffness curves must be used. In order to use these curves it is necessary to assume the existence of a reasonably straight elastic axis. The location of this axis may be estimated by considering it to be the line connecting the shear centers of the individual sections. If the elastic axis obtained in this manner is not reasonably straight within a few percent of the chord, the results of the analysis may not be sufficiently reliable.

The stiffnesses  $GJ$  and  $EI$  do not have much physical significance inboard of the last point where there is a complete cross section of the torsion box. (See fig. 1.) In order to arrive at estimates of the root stiffnesses  $(GJ)_r$  and  $(EI)_r$ , which serve primarily as reference values in this analysis, the stiffness curves have to be extended. It is convenient to consider the stiffnesses to be constant inboard of the last complete section of the torsion box; this procedure should yield conservative values of the root rotations.

The most difficult problem incurred in analyzing the deflections on the basis of stiffness curves appears to be the estimation of the root rotations. As used in this analysis, they are the torsion and bending deflections imposed by the triangular inner portion of the wing and the carry-through bay on the rest of the wing. As seen in figure 2, which is plotted from the data of reference 5, these values are essentially constant along the span, so that they actually constitute rigid-body rotations. (The bending rotations have been obtained by taking the difference in slope between curves calculated by considering the wing to be cantilevered at the effective root - the root used to calculate torsional deformations in reference 5 - and the averages of the leading-edge and trailing-edge deflections actually measured. The twists were obtained by subtracting the twists calculated on the basis of the assumed effective root from the measured twists.)

The rotations should in any practical case be calculated by analyzing the triangular root and the carry-through bay and made dimensionless by means of equations (9). If such an analysis is not available, the dimensionless rotation parameters shown in figure 2 may be used as a guide; it must be kept in mind, however, that in the case of a sweptforward wing the parameters  $Q_{\theta M}$  and  $Q_{\theta T}$  would have the opposite sign.

Once the structure under investigation is built, fairly simple deflection tests, similar to those performed in reference 5, may be used to check the root-rotation parameters by calculating the differences between the observed rotations and those calculated by simple beam theory considering the wing cantilevered at the effective root; at the same time the existence and estimated location of the elastic axis may be verified. If the experimental program is fairly extensive it is desirable to measure influence coefficients directly. These influence coefficients can then be used in conjunction with the alternate method described in the preceding section to obtain a quick check on the aeroelastic analysis based on calculated stiffnesses.

The influence coefficients used in the analysis consist of the rotations of sections parallel to the direction of flight due to concentrated unit torques in planes parallel to the plane of symmetry



or concentrated unit loads at the reference line. These rotations in radians are entered in tables of the form:

$$[\phi_R]$$

TWIST AT STATION  $y/s_w$  DUE TO  
UNIT CONCENTRATED TORQUE AT

$$y_1/s_w$$

$y_1/s_w \backslash y/s_w$	0.2	0.4	0.6	0.8	0.9	1.0
0						
0.2						
0.4						
0.6						
0.8						
0.9						

$$[\phi_P]$$

TWIST AT STATION  $y/s_w$  DUE TO  
UNIT CONCENTRATED LOAD AT

$$y_1/s_w$$

$y_1/s_w \backslash y/s_w$	0.2	0.4	0.6	0.8	0.9	1.0
0						
0.2						
0.4						
0.6						
0.8						
0.9						

These particular tables would be used for a six-point analysis; similar tables would be used for a ten-point analysis. In either case it is to be noted that the twists are measured at values of  $y/s_w$  from 0 to 0.9, whereas the loads are applied at  $y_1/s_w$  values from 0.2 to 1.0. The tables obtained in this manner constitute the desired influence-coefficient matrices.

If the wing sections are found to twist nonuniformly, so that they become cambered in effect, the angles of twist  $\alpha_s$  to be entered in the influence-coefficient matrices have to be defined in a different manner according to whether the aeroelastic analysis is performed for subsonic or supersonic speeds. At subsonic speeds the lift depends on the slope of the mean camber line at the three-quarter-chord point, so that the effective angle of attack is

$$\alpha_s = 2 \frac{(\zeta_c - \zeta_{TE})}{c} \quad (30)$$

At supersonic speeds the lift depends primarily on the average slope of the mean camber line, so that

$$\alpha_s = \frac{\zeta_{LE} - \zeta_{TE}}{c} \quad (31)$$

#### Determination of the Aerodynamic Parameters

The selection of the aerodynamic parameters  $m_0$  and  $e_1$  for the calculation of the divergence speed has been discussed in reference 3. For calculating the aerodynamic loading at a given flight condition the aerodynamic parameters are chosen for that flight condition. The effective lift-curve slopes  $m_0$  and  $m_{e1}$  are applicable only to subsonic subcritical speeds. At higher speeds no simple span correction is available; neglect of the span correction tends to be conservative for calculation of the divergence speed and the aerodynamic loading, however.

#### Instructions for Solution

Two sets of integrating matrices have been prepared, one for a six-point solution and one for a ten-point solution. The former should be adequate for all practical purposes; only where the stiffness curves are very irregular near the root does the ten-point solution have to be resorted to. The points considered by the two sets of tables are at

$\frac{\eta}{s_A} = 0, 0.2, 0.4, 0.6, 0.8, \text{ and } 0.9$  for the shorter solution and

$\frac{\eta}{s_A} = 0, 0.1, 0.2, 0.3, 0.4, 0.5, 0.6, 0.7, 0.8, \text{ and } 0.9$  for the longer

solution. The procedure to be followed for either solution is identical; although computing forms are presented in this paper only for the six-point solution, their extension to apply to the ten-point solution is obvious.

Calculation of the matrices.— The first step in the aeroelastic analysis by means of the stiffness curves is the calculation of the aeroelastic matrix  $[A]$  from the physical and geometrical parameters of the wing. These parameters are conveniently tabulated in a form of the type shown in table VI(a). The computation is then carried out according to the instructions of table VI(b), each step in the procedure being identified by the number in the upper left corner of each box. It must be kept in mind that many of the operations call for matrix multiplications where the order of the multiplicands is of importance. (A brief summary of matrix methods is presented in the appendix.) The aeroelastic matrix is obtained as the last step (step 13) of the computations in this form which constitutes an evaluation of the  $A$  matrix given in equation (15).

A special case arises when  $e_{1r}$  is zero. If  $e_1$  is not zero along the remainder of the span, its value at some point other than the root may be used as a reference value. The  $\left[ \frac{e_1}{e_{1r}} \left( \frac{c}{c_r} \right)^2 \right]$  matrix and the multiplying factors of steps 8 and 9 as well as the definition of the parameter  $a$  are then based on this other reference value rather than  $e_{1r}$ . If  $e_1$  is zero along the entire span, step 1 and steps 3 to 8 may be omitted and steps 9 to 13 should be modified as follows:

- Step 9  $\frac{(EI)_r}{(GJ)_r} \frac{w}{s_w \tan \Lambda} \frac{Q_{QM}}{[I_o]}$
- Step 10  $[9] - [2]$
- Step 11 As is
- Step 12 Omit
- Step 13  $[A]_{e_1=0} = [10] [11]$

If influence coefficients of the proper type are available, the calculation of the aeroelastic matrix  $[A']$  is carried out directly by means of equation (28).

Solution for divergence dynamic pressure.— In order to determine the value of the parameter  $a$  or  $a'$  corresponding to divergence, the aeroelastic matrix  $[A]$  or  $[A']$  is iterated (see appendix) as indicated by equation (18). Table VII(a) may be used for this purpose. The result is the critical value of  $a$  or  $a'$ . The divergence dynamic pressure is then calculated from equation (16) or (27). It is to be noted that this pressure will be in pounds per square inch. Since the aeroelastic matrix is independent of the Mach number, except insofar as  $e_1$  varies with Mach number, the same critical value of  $a$  may be used to calculate the divergence dynamic pressure for an entire range of Mach numbers. If the value of  $e_1$  changes, however, as it does between the subsonic and supersonic region, the critical value of  $a$  has to be calculated for both values of  $e_1$ .

If the value of  $e_1$  is zero along the entire span and the  $[A]$  matrix has been calculated according to the modified instructions, iteration of the matrix will give the value of the parameter  $d$  at divergence. From the definition of  $d$  the divergence dynamic pressure may then be calculated.

Solution for aerodynamic loading.— In order to calculate the aerodynamic loading corresponding to a given flight condition and geometric angle-of-attack distribution the aeroelastic matrix  $[A]$  or  $[A']$  is multiplied by the value of  $a$  or  $a'$  calculated for the given flight condition and subtracted from the unit matrix  $[I]$ . (See equation (17).) The result may be entered in table VII(b). Again it must be noted that the value of the aeroelastic matrix varies with the flight condition if  $e_1$  varies, so that the aeroelastic matrix corresponding to the proper  $e_1$  value must be selected. The resulting matrix constitutes the coefficients of a set of simultaneous linear algebraic equations for the unknown values of the effective angle-of-attack distribution of the deformed wing

$\left\{ \frac{m_e}{m_{e1}} \bar{\alpha} \right\}$  in terms of the known angle-of-attack values of the rigid wing  $\{\alpha_g\}$ . Table VII(b) is set up for the calculation of the additional loading, the damping-in-roll loading, and a third arbitrary loading; as many loadings as desired may, of course, be calculated by this method. The solution of the equations may be carried out in any convenient manner. The form of table VII(b) has been prepared for use in conjunction with Crout's method of solving linear simultaneous equations (reference 6).

In the case where  $e_1$  is zero along the span, the headings at the top of table VII(b) should be modified to read

$$\frac{d}{dD} = \text{---} \quad d = \text{---}$$

$$[I] - d[A]_{e_1=0}$$

where  $[A]_{e_1=0}$  has been calculated according to the modified instructions and  $d$  has been obtained by iterating  $[A]_{e_1=0}$ .

The values of  $\left\{ \frac{m_e}{m_{e1}} \bar{\alpha} \right\}$  calculated for the additional load distribution ( $\alpha_g = 1$ ) constitute values of the ratio  $c_{l_{fw}}^*/c_{l_{rw}}$  or  $(cc_l)_{fw}/(cc_l)_{rw}$  in view of the assumptions made concerning the air forces. The section loading of the flexible wing is obtained from the relation

$$cc_l = cm_{e1} \left( \frac{m_e}{m_{e1}} \bar{\alpha} \right) \quad (32)$$

or in dimensionless form

$$\frac{cc_l}{c_r} = m_{e1} \frac{c}{c_r} \left( \frac{m_e}{m_{e1}} \bar{\alpha} \right) \quad (32a)$$

The wing lift coefficient defined by the relation

$$C_{L_w} = \frac{L_w}{qS} \quad (33)$$

and the wing bending-moment coefficient defined by

$$C_{BM_w} = \frac{M^* r}{qSb} \quad (34)$$

may be obtained by integrating the load distribution. These integrations may be performed conveniently by multiplying the  $cc_l/c_r$  values by the first rows of the  $[K_1]$  and  $[K_2]$  matrices, respectively. Thus

$$C_{L_w} = \frac{s_w c_r}{S/2} [K_1]_1 \left\{ \frac{cc_l}{c_r} \right\} \quad (35)$$

$$= m_{e1} \frac{s_w c_r}{S/2} [K_1]_1 \left[ \frac{c}{c_r} \right]_1^0 \left\{ \frac{m_e}{m_{e1}} \bar{\alpha} \right\} \quad (35a)$$

and

$$C_{BM_w} = \frac{s_w c_r}{S/2} \frac{s_w}{2b} [K_2]_1 \left\{ \frac{cc_l}{c_r} \right\} \quad (36)$$

$$= m_{e1} \frac{s_w c_r}{S/2} \frac{s_w}{2b} [K_2]_1 \left[ \frac{c}{c_r} \right]_1^0 \left\{ \frac{m_e}{m_{e1}} \bar{\alpha} \right\} \quad (36a)$$

The lateral center of pressure of the wing load  $\frac{\bar{y}}{s_w}$  may then be determined from the relation

$$\frac{\bar{y}}{s_w} = \frac{2b}{s_w} \frac{C_{BM_w}}{C_{L_w}} \quad (37)$$

The fore-and-aft location of the aerodynamic center of the wing load measured rearward of the leading edge of the mean aerodynamic chord as a fraction of the mean aerodynamic chord may be estimated from the relation

$$\frac{(ac)_w}{c_{MAC}} = ac + \frac{\bar{y} - y_{MAC}}{c_{MAC}} \tan \Lambda_{ac} \quad (38)$$

where  $\Lambda_{ac}$  is the sweep of the section-aerodynamic-center line.

For any other geometrical angle-of-attack distributions such as those due to built-in twist or those due to rolling, the same section lift-curve slope should be used as for the structural deformations, so

that  $m_{e1}$  is replaced by  $m_e$  and  $\frac{m_e}{m_{e1}}$  is unity in equations (32), (35), and (36). For the damping-in-roll distribution with a tip helix angle of 1 radian

$$\alpha_g = 1 - \frac{s_w}{b/2} \left( 1 - \frac{\eta}{s_\Lambda} \right) \quad (39)$$

The rolling-moment coefficient due to the wing load is defined by

$$C_{l_w} = \frac{2M^* r}{qSb} \quad (40)$$

It is seen to be twice the wing bending-moment coefficient.

The contribution of the wing to other stability derivatives may be obtained similarly by integrating the load distributions due to the angle-of-attack distributions caused by the motion under consideration, as described in reference 7; in the case of swept wings, particular care must be taken in selecting the proper angle-of-attack distribution and in accounting for the lateral inclination of the lift vector. (See reference 4.)

If the aerodynamic loading or the stability derivatives are to be obtained for a wide variety of flight conditions, it is convenient to

systematize the calculations in the following manner: The aeroelastic matrix is computed for both the subsonic and supersonic aerodynamic-center values and iterated for both cases to obtain the subsonic and supersonic values of the divergence parameter  $a_D$ . From these values the divergence dynamic pressure may be computed by means of equation (15) and plotted against Mach number, as suggested in reference 3; on the same plot values of the actual dynamic pressure may be plotted against Mach number for various altitudes of interest. Such a plot for a wing, the physical characteristics of which are given in figure 3, is shown in figure 4.

Since at a given Mach number the ratio  $a/a_D$  is equal to the ratio  $q/q_D$ , the range of  $a/a_D$  values of interest may be established from this plot for both the subsonic and the supersonic region. Several representative  $a/a_D$  values may then be chosen within the given ranges and the corresponding values of  $a$  computed from the previously calculated  $a_D$  values. The aerodynamic loading is calculated for these values of  $a$  using the appropriate  $[A]$  matrix and plotted in the form of  $(cc_l)_{fw}/(cc_l)_{rw}$ , with the ratio  $a/a_D$  as a parameter. From these curves or from the  $\frac{m_e}{m_{e1}} \bar{\alpha}$  values the lift coefficients may be obtained in the form  $(C_L)_{fw}/(C_L)_{rw}$  and plotted against  $a/a_D$  or  $q/q_D$ ; the other coefficients may be obtained and plotted in a similar form.

For any specific flight condition the value of  $a/a_D$  may then be obtained from the plot of  $q$  and  $q_D$  against Mach number. The loading, lift coefficient, or other item of interest may be obtained from the plots which give these items in terms of the rigid-wing values. Once the rigid-wing values at the given Mach number are known, the flexible-wing values may then be obtained immediately.

#### Illustrative Example

In order to illustrate the method described in the preceding sections, a typical swept wing has been analyzed. The physical and geometrical parameters of the wing are shown in figure 3 and the upper part of table VIII (which follows the form of table VI(a)). The chord,  $e_1 c^2$ , and stiffness matrices have been obtained from the given parameters and are shown in the lower part of table VIII.

The calculation of the aeroelastic matrix for the subsonic case has been carried out by means of the form of table VI(b). All but three of the steps of the computation are shown in table IX numbered in the same order as in table VI(b). Steps 1, 2, 6, 7, 11, and 12 constitute matrix multiplications, which are carried out in the order

indicated; steps 5 and 13 constitute matrix additions or subtractions; steps 3 and 4 constitute multiplications of matrices by constants.

The aeroelastic matrix is iterated in table X(a) (which follows the form of table VII(a)) to yield a value of  $a_D = -2.208$ . From this value and a value of  $a_D$  computed in the same manner for supersonic speeds, the divergence dynamic pressure has been calculated by means of equation (16) on the basis of estimated values of the effective lift-curve slope. The variation with Mach number of the divergence dynamic pressure, the actual dynamic pressure at sea level, and the estimated effective lift-curve slope is shown in figure 4.

For a value of  $\frac{a}{a_D} = -0.25$ , such as would be obtained approximately at a Mach number of 1.0, the aerodynamic loading has been calculated for the additional-angle-of-attack case and the damping-in-roll case in table X(b), which follows the form of table VII(b). The values of  $\alpha_g$  for the damping-in-roll case have been calculated from equation (39). The aerodynamic loadings, in addition to those calculated for other  $q/q_D$  values, have been plotted in figure 5 as ratios of the flexible-wing loadings to the rigid-wing loadings. The curves have been integrated to yield wing lift and rolling-moment coefficients as well as the aerodynamic center of the wing load, which are shown in table X(b) for the case of  $\frac{a}{a_D} = -0.25$  and which are plotted against  $-\frac{q}{q_D}$  in figure 6.

The wing lift coefficient is defined in such a manner that if the fuselage lift is known and made dimensionless by dividing by  $q$  and  $S$  the resulting fuselage lift coefficient may be added directly to the wing lift coefficient. This definition and the fact that figure 5(a) is plotted over the fraction of the wing-alone span  $s_w$  explain the fact that the area under the curve of figure 5(a) is not 1. The aerodynamic center as plotted in figure 6 constitutes the center of pressure of only the wing load. In order to obtain the airplane aerodynamic center, the magnitude and center of pressure of the fuselage load would have to be known and taken into account.

#### DISCUSSION

Both the aerodynamic and the structural assumptions made in this analysis are more realistic than those made in reference 3. The device employed in this analysis of calculating the air forces for wing sections parallel to the direction of flight and then transferring them to sections perpendicular to the elastic axis obviates the necessity of



replacing the actual wing with one the root and tip of which are perpendicular to the elastic axis for the purpose of analysis. Furthermore, the inclusion of Falkner's modification (see appendix) in the integrating matrices has the effect of rounding off the load distribution approximately in the manner observed at subsonic speeds. At supersonic speeds the load distributions do not go to zero in the manner assumed in Falkner's modification, but even at supersonic speeds there is some reduction of load at the tip, the total magnitude of which is not far from the reduction obtained by Falkner's modification.

Only one aerodynamic assumption is still made: that induction effects may be approximated by an over-all reduction of the strip theory loading (rounded off as previously described) at subcritical speeds and may be neglected at supersonic speeds. The effects of aerodynamic induction could be taken into account more accurately by using aerodynamic influence-coefficient matrices instead of the effective lift-

curve-slope concept and the  $\begin{bmatrix} \frac{c}{c_r} \end{bmatrix}$  and  $\begin{bmatrix} \frac{e_1}{e_{1r}} \left( \frac{c}{c_r} \right)^2 \end{bmatrix}$  matrices used in

this analysis. Available methods of calculating such influence coefficients for wings of arbitrary plan form at subsonic and supersonic speeds, particularly those suitable for wings with large amounts of sweep, are either too inaccurate or too time-consuming for practical purposes, however.

Although the analysis of this paper has been performed for wings consisting of uncambered sections, it is directly applicable as well to the determination of the additional loading of wings with cambered sections. The loading of such wings due to the section pitching moment at zero lift may be determined by modifying the analysis somewhat.

The assumption of an effective root perpendicular to the elastic axis made in reference 3 for the purposes of calculating the structural response is carried over in this analysis. It is modified, however, to the extent that the root is no longer considered to be rigid as in reference 3, but flexible, both in torsion and bending. It has been demonstrated in reference 5 that the deflections of a swept beam may be estimated on that assumption, provided the root-rotation parameters are known. By assuming the effective root at the intersection of the elastic axis with the side of the fuselage, the root bending due to bending moment and root twist due to torque are minimized. The bending due to twist and twist due to bending are the same regardless of the location of the effective root.

The method of introducing the root rotations into the analysis by means of the  $[I_0]$  matrix assures that the structural twist in planes parallel to the direction of flight is zero at the fuselage. From

figure 2 it is seen that the local values of the root rotation either tend to approach zero at the root or tend to cancel each other. If the root-rotation constants are known, the structural deformations can therefore be predicted quite accurately by the assumptions made.

The manner in which the equations of equilibrium are solved by means of the integrating matrices accounts for the true chord and stiffness variations. It does not necessitate replacement of the actual wing by constant-chord segments with all the flexibility concentrated at the ends of the segments, an approach which has been used extensively in the work on aeroelastic problems of straight wings.

A further refinement which obviates the necessity for making any structural assumptions other than that of small deflections is the use of measured influence coefficients in the aeroelastic analysis. Wherever such coefficients are available it is, of course, of advantage to use them.

No explicit account has been taken in the analysis of the effects of the inertia loading on the structural deformations and hence the aerodynamic loading. On swept wings, in particular, their effects may be considerable. For the purposes of this analysis, however, the structural deformations due to inertia loading may be considered part of the geometric angle of attack and the rigid-wing geometric angle of attack may be modified accordingly. The deformations due to the inertia loading may, incidentally, be calculated conveniently by means of the  $K_1$ ,  $K_2$ , and  $K_3$  matrices.

Some of the general observations made in reference 3 concerning the divergence phenomenon are corroborated by the example. As expected of a wing with a considerable amount of sweepback, the divergence dynamic pressure is negative. Consequently the wing cannot diverge. The divergence dynamic pressure is useful as a reference value, however; the values of the load distribution and the stability parameters divided either by the corresponding rigid-wing values or by the section lift-curve slope depend only on the ratio of the actual to the divergence dynamic pressure.

The type of plot shown in figure 4 is therefore quite useful in the analysis of aeroelastic phenomena. As pointed out in reference 3, this chart may also be used to estimate the actual divergence dynamic pressure where there is a possibility that the wing may diverge. It appears that the critical values will occur at either extremity of the transonic region. In the transonic region proper the lift-curve slope usually appears to be lower than at the extremities, so much so that the decrease in lift-curve slope even tends to overbalance any forward shift in aerodynamic center.

As would be expected qualitatively, the effect of wing flexibility in the case of the example wing is to unload the wing tips owing to the fact that they bend up. The lift carried by the wing is therefore less than that carried by a rigid wing, the center of pressure being farther inboard and the aerodynamic center farther forward.

The difference between the supersonic and subsonic values of the loading, the lift and rolling-moment coefficients, and the aerodynamic center for a given value of  $a/a_D$  is due to the difference in the  $e_1$  distributions. If the distributions were the same, the subsonic and supersonic variations of these quantities with  $a/a_D$  would coincide despite the difference in the  $e_{1r}$  values.

Another item of possible interest is the fact that the variations of the parameters  $d_D$  and  $a_D$  for the example problem are approximately linear (see fig. 7), as would be expected from the results of the analysis of reference 3. The deviations from linearity are most pronounced near the points for  $d = 0$  (that is,  $\Lambda = 0^\circ$ ). They are due to the effects of the root rotations, in particular, the bending due to torsion and torsion due to bending; these effects were neglected in the approximate analysis of reference 3. The points of figure 7 correspond to the example wing and the wings that would be obtained by rotating the example wing to the unswept and  $37.5^\circ$  sweptforward positions in such a manner as to keep the parameters  $\frac{e_{1r} c_r \cos \Lambda}{s_\Lambda}$ ,  $\frac{(EI)_r}{(GJ)_r}$ , as well as the chord, stiffness, and moment-arm ( $e_1$ ) distributions constant. Points are shown for both the subsonic and supersonic variations as well as for the case when  $e_1 = 0$  over the entire span ( $a_D = 0$ ). The difference between the subsonic and supersonic lines is due entirely to the difference in the  $e_1$  distribution; if the distributions were the same, as would be the case if the elastic axis were at a constant fraction of the chord, the variations would be the same, regardless of the difference in the  $e_{1r}$  values.

The present analysis is concerned only with wing or tail loads; the total loads are obtained by adding the fuselage loads (which may be assumed to be unaffected by flexibility) to the wing or tail loads obtained from the analysis. The amount of load carried by a flexible wing and the manner of its distribution can consequently be estimated by the method presented herein if the contribution of the fuselage is known at low dynamic pressures, that is, for the "rigid-wing" case.

The fuselage has a considerable effect on some of the stability parameters as well, although in the case of others, such as  $C_{L_p}$ , the effect is negligible. Other effects that may have to be accounted for in calculating stability derivatives are the boundary-layer behavior and tip suction. The boundary-layer effect may be accounted for by using a section lift-curve slope corrected for boundary-layer effects to calculate the angle-of-attack distribution of the flexible wing at the flight conditions of interest and then obtaining the lift and drag distributions corresponding to that angle-of-attack distribution. Lateral tip suction may be important on low-aspect-ratio and highly swept wings. Since it does not affect the lift distribution, it may be taken into account by calculating the angle-of-attack distribution of the flexible wing and estimating the tip suction corresponding to the actual angle of attack at the tip.

In calculating stability derivatives it is well to keep in mind that the method presented in this paper is based on a modified strip theory, unless aerodynamic influence-coefficient matrices are used. The calculated derivatives may therefore be somewhat in error, particularly if in calculating them the moment of a load distribution has to be determined. If there is reason to suspect that the modified strip theory is inadequate for calculating a given derivative, the derivative may be calculated for the rigid-wing case by a more refined method; the results calculated by the method of this paper may then be used to correct the accurate rigid-wing value for the effect of structural flexibility.

#### CONCLUDING REMARKS

A method has been presented for calculating the aerodynamic loading, the divergence speed, and certain stability derivatives of wings and tail surfaces of arbitrary plan form and stiffness. Provisions have been made for using either stiffness curves and root-rotation constants or influence coefficients in the structural part of the analysis. Strip theory with over-all reduction and rounding off at the tip to take account of aerodynamic induction have been used for the aerodynamic part of the analysis. Computing forms, tables of numerical constants required in the analysis, and an illustrative example are included to facilitate calculations by means of the method.

Langley Aeronautical Laboratory  
National Advisory Committee for Aeronautics  
Langley Air Force Base, Va., December 24, 1948

## APPENDIX

## SUMMARY OF MATRIX ALGEBRA PERTINENT TO THE ANALYSIS

For the convenience of the reader unfamiliar with matrix terminology, a summary of matrix definitions and methods is presented in the following sections. For a more complete discussion of matrix methods the reader is referred to any text on matrices, for instance reference 8.

## Definitions

A matrix is a rectangular array of numbers, called elements, written down in rows and columns. A column matrix consists of a single column, a row matrix of a single row. A square matrix has as many rows as it has columns. The diagonal of a square matrix from the upper left to the lower right is called the principal diagonal. A matrix all the elements of which are zero except for those on the principal diagonal is called a diagonal matrix. If all of these elements are unity, the matrix is termed the unit matrix.

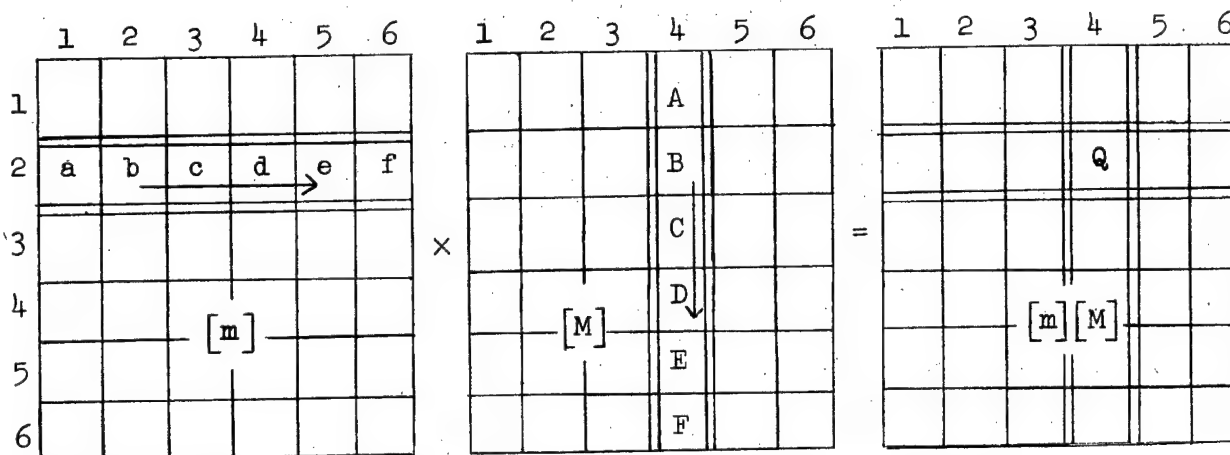
## Matrix Algebra

Addition.— Two matrices can be added or subtracted if both have the same number of rows and columns. The addition or subtraction is carried out by adding to or subtracting from each element of the first matrix the corresponding element of the second matrix.

Multiplication by a constant.— A matrix is multiplied by a constant by multiplying each element by that constant.

Matrix multiplication.— Two matrices can be multiplied by each other if the second has as many rows as the first has columns. The elements of the resulting matrix are obtained by multiplying the elements in the corresponding row of the first matrix by those of the corresponding column of the second matrix in the following order: The first element of the row is multiplied by the first element of the column, the second by the second, and so forth. The sum of the products obtained in this

manner is the value of the element of the product matrix. Schematically this process may be illustrated as follows:



$$Q = aA + bB + cC + dD + eE + fF$$

It must be emphasized that in multiplying matrices by each other their order is of importance. As the two matrices under consideration are written the matrix at the left (the  $m$  matrix) is said to be post-multiplied by the other, (the  $M$  matrix); or the  $M$  matrix may be said to be premultiplied by the  $m$  matrix, in order to distinguish the manner in which they are multiplied. If the two matrices were written in the reverse order and then multiplied according to the foregoing instructions, that is, if the  $[M]$  matrix were postmultiplied by the  $[m]$  matrix, the element of the second row and fourth column of the product matrix  $[M][m]$  would clearly not have the value  $Q$  in general, nor would, in general, any other element have the value it would have if the two matrices were multiplied in the order shown. Consequently it is important to observe the order in which the matrices are written down in the computing instructions.

**Matrix iteration.**— The purpose of iterating a square matrix is to determine the column matrix or matrices which, if postmultiplied by the given square matrix, yield the same column matrix except for a constant multiplier. It is the value or values of these multipliers which constitute the desired characteristic values of the matrix.

The iteration is carried out by assuming a "trial" column (the column shown in table VII is convenient for the purpose of this analysis) and premultiplying it by the given square matrix to yield a "result" column. The elements of the result column including the last are divided by the last element of the result column and entered as a second trial column. The second trial column is then premultiplied by the square matrix to yield a second result column. The procedure is

repeated until the same value (within the desired accuracy) is obtained twice in succession for the last element of the result matrix. The reciprocal of this value is the desired (lowest) characteristic value of the matrix, that is, the lowest critical value of  $a_D$ , in the analysis of this paper.

Another way of estimating a first trial column in this analysis is to add the elements in each row of the A matrix, enter the six sums in the first result column, and treat them as if they had been obtained by multiplying the A matrix by a first trial column.

### Derivation of the Integrating Matrices

Although familiarity with the derivation of the integrating matrices is not essential to the application of the method of this paper, an outline of the derivation is presented because of its general interest.

The integrating matrices used in this paper are based on the same concept as Simpson's rule - replacement of the actual function which is to be integrated by parabolic segments. If the function  $y$  has the values  $y_{n-1}$ ,  $y_n$ , and  $y_{n+1}$ , respectively, at the equally spaced points  $x_{n-1}$ ,  $x_n$ , and  $x_{n+1}$ , the following relations are seen to be true for a second-degree parabola passed through the three known points:

$$y = y_n + \frac{1}{2}(y_{n+1} - y_{n-1})(x - x_n) + \frac{1}{2}(y_{n+1} - 2y_n + y_{n-1})(x - x_n)^2 \quad (A1)$$

$$\int_{x_{n-1}}^{x_{n+1}} y \, dx = \left(\frac{1}{3} \Delta x\right) y_{n-1} + \left(\frac{4}{3} \Delta x\right) y_n + \left(\frac{1}{3} \Delta x\right) y_{n+1} \quad (A2)$$

$$\int_{x_n}^{x_{n+1}} y \, dx = \left(-\frac{1}{12} \Delta x\right) y_{n-1} + \left(\frac{2}{3} \Delta x\right) y_n + \left(\frac{5}{12} \Delta x\right) y_{n+1} \quad (A3)$$

$$\int_{x_{n-1}}^{x_n} y \, dx = \left(\frac{5}{12} \Delta x\right) y_{n-1} + \left(\frac{2}{3} \Delta x\right) y_n + \left(-\frac{1}{12} \Delta x\right) y_{n+1} \quad (A4)$$

$$\int_{x_{n-1}}^{x_{n+1}} (x - x_n) y \, dx = \left(-\frac{1}{3} \Delta x^2\right) y_{n-1} + (0) y_n + \left(\frac{1}{3} \Delta x^2\right) y_{n+1} \quad (A5)$$

$$\int_{x_n}^{x_{n+1}} (x - x_n) y \, dx = \left(-\frac{1}{24} \Delta x^2\right) y_{n-1} + \left(\frac{1}{4} \Delta x^2\right) y_n + \left(\frac{7}{24} \Delta x^2\right) y_{n+1} \quad (A6)$$

where

$$\Delta x = x_n - x_{n-1} = x_{n+1} - x_n \quad (A7)$$

The different integrations over the parabolic segments may thus be performed by multiplying the given  $y$  values by the multiplying factors indicated in equations (A2) to (A6).

Since load distributions at subsonic speeds go to zero with infinite slope at the tip and the ordinary second-degree parabola furnishes a poor approximation to such a distribution, V. M. Falkner has suggested that a curve of the type

$$y = A_0 + A_1(1 - x)^{1/2} + A_2(1 - x)^{3/2} \quad (A8)$$

be passed through the last three points of the load-distribution curve at the tip ( $x = 1$ ). On the basis of the approximation, relations equivalent to equations (A1) to (A6) may be derived. The multiplying factors for the last two segments are then based on these equivalent expressions rather than those of equations (A2) to (A6).

The integrating factors of equations (A2) to (A6) may be assembled directly into integrating matrices. The  $K_3$  matrix, for instance, is set up to perform the integration  $\int_0^x y \, dx$ . If at the upper limit  $x = 0.1$  and if the ten-point matrix (table III(b)) is to be used, the factors 0.04167, 0.06667, and -0.00833 may be obtained from equation (A4) since  $x_{n-1} = 0$ ,  $x_n = 0.1$ , and  $\Delta x = 0.1$ ; similarly, if for the same case the integration is extended to  $x_{n+1} = 0.2$  as the upper limit, the integrating factors 0.03333, 0.13333, and 0.03333 will be obtained from equation (A2). These factors constitute the second and third rows of the matrix  $K_3$ ; since the integrations are independent of the  $y$  values other than the first three, the other  $y$  values are multiplied by zero in these two rows. In order to extend the integration to  $x = 0.3$  an integration is



again performed up to  $x = 0.2$  and another integration, using another parabolic segment, is performed from  $x = 0.2$  to  $x = 0.3$ . For the latter integration  $x_{n-1} = 0.2$ ,  $x_n = 0.3$ , and  $\Delta x = 0.1$ , so that equation (A4) again yields the factors 0.04167, 0.06667, and -0.00833. The  $y$  value at  $x = 0.2$  is therefore assigned a multiplying factor of 0.03333 by the first integration and a factor of 0.04167 by the second, or a total factor of 0.07500. The resulting factors are entered in the fourth row of the  $K_3$  matrix. All other rows are obtained in a similar manner.

The  $K_1$  matrix is set up to perform the integration  $\int_x^1 y \, dx$ . The values of the last row of the ten-point  $K_1$  matrix (table I(b)) are obtained from Falkner's equivalent of equation (A3) for the curves assumed in reference 5, with  $x_{n-1} = 0.8$ ,  $x_n = 0.9$ ,  $x_{n+1} = 1.0$ , and  $\Delta x = 0.1$ . Only the multiplying factors for the  $y$  values at  $x = 0.8$  and  $x = 0.9$  are listed, since the  $y$  value at  $x = 1.0$  (the wing tip) is assumed to be zero in this analysis, so that its multiplying factor is immaterial. The values of the last row but one are obtained similarly from Falkner's equivalent of equation (A2). The values of the row for  $\frac{\eta}{s_\Lambda} = 0.7$  are obtained by using equation (A3) in the interval  $x = 0.6$  to  $x = 0.8$  and Falkner's equivalent of equation (A2) in the interval  $x = 0.8$  to 1.0. Similarly the row for  $\frac{\eta}{s_\Lambda} = 0.6$  is obtained by combining the results of equation (A2) for the interval  $x = 0.6$  to 0.8 with Falkner's equivalent of equation (A2) for the interval  $x = 0.8$  to 1.0. All other rows are obtained in a similar manner.

The  $K_2$  matrix is set up to perform the integration  $\int_{x_0}^1 (x - x_0)y \, dx$ , where  $x$  is the variable of integration and  $x_0$  the value of  $x$  at the lower limit. In applying the integrating factors of equations (A2) through (A6) to this integration it must be realized that

$$\int (x - x_0)y \, dx = (x_n - x_0) \int y \, dx + \int (x - x_n)y \, dx \quad (A9)$$

so that the integrating factors for this integration would be obtained by adding  $(x_n - x_0)$  times the factors of equation (A2) or (A3) to the factors of equation (A5) or (A6), respectively, depending on the limits of the integration. The factors for the different segments ( $x = 0.8$  to 1.0, 0.6 to 0.8, and so forth) are then combined for any given row (with its given value of  $x_0$ ) in the manner indicated for the  $K_1$  matrix to yield the  $K_2$  matrix.

The  $K_4$  matrix sums up the torques outboard of a given point, while the  $K_5$  matrix gives the sum of the moments of forces applied outboard of a given point. Neither requires any integrations in the sense of equations (A2) to (A6). For the six-point method these two matrices are:

 $K_4$ 

$y/s_w$	0.2	0.4	0.6	0.8	0.9	1.0
0	1	1	1	1	1	1
0.2	0	1	1	1	1	1
0.4	0	0	1	1	1	1
0.6	0	0	0	1	1	1
0.8	0	0	0	0	1	1
0.9	0	0	0	0	0	1

 $K_5$ 

$y/s_w$	0.2	0.4	0.6	0.8	0.9	1.0
0	0.2	0.4	0.6	0.8	0.9	1.0
0.2	0	.2	.4	.6	.7	.8
0.4	0	0	.2	.4	.5	.6
0.6	0	0	0	.2	.3	.4
0.8	0	0	0	0	.1	.2
0.9	0	0	0	0	0	.1

It will be noted that the moment arms which comprise the  $K_5$  matrix are fractions of  $s_w$ , so that the matrix must be multiplied by the length  $s_w$  in order to yield actual moments as stated in equation (21).

## REFERENCES

1. Reissner, H.: Neuere Probleme aus der Flugzeugstatik. Z.F.M., Jahrg. 17, Heft 7, April 14, 1926, pp. 137-146.
2. Flax, Alexander H.: The Influence of Structural Deformation on Airplane Characteristics. Jour. Aero. Sci., vol. 12, no. 1, Jan. 1945, pp. 94-102, 117.
3. Diederich, Franklin W., and Budiansky, Bernard: Divergence of Swept Wings. NACA TN No. 1680, 1948.
4. Toll, Thomas A., and Queijo, M. J.: Approximate Relations and Charts for Low-Speed Stability Derivatives of Swept Wings. NACA TN No. 1581, 1948.
5. Zender, George, and Libove, Charles: Stress and Distortion Measurements in a  $45^\circ$  Swept Box Beam Subjected to Bending and to Torsion. NACA TN No. 1525, 1948.
6. Crout, Prescott D.: A Short Method for Evaluating Determinants and Solving Systems of Linear Equations with Real or Complex Coefficients. Trans. A.I.E.E., vol. 60, 1941, pp. 1235-1241.
7. Pearson, Henry A., and Jones, Robert T.: Theoretical Stability and Control Characteristics of Wings with Various Amounts of Taper and Twist. NACA Rep. No. 635, 1938.
8. Frazer, R. A., Duncan, W. J., and Collar, A. R.: Elementary Matrices and Some Applications to Dynamics and Differential Equations. The Macmillan Co., 1946.

TABLE I.— VALUES OF THE INTEGRATING MATRIX  $[K_1]$ 

## (a) Six-Point Solution

$\eta/s_\Delta$	0	.2	.4	.6	.8	.9
0	0.06667	0.26667	0.13333	0.26667	0.09333	0.15085
.2	-.01667	.13333	.15000	.26667	.09333	.15085
.4	0	0	.06667	.26667	.09333	.15085
.6	0	0	-.01667	.13333	.11000	.15085
.8	0	0	0	0	.02667	.15085
.9	0	0	0	0	-.01886	.09333

## (b) Ten-Point Solution

$\eta/s_\Delta$	0	.1	.2	.3	.4	.5	.6	.7	.8	.9
0	0.03333	0.13333	0.06667	0.13333	0.06667	0.13333	0.06667	0.13333	0.06000	0.15085
.1	-.00833	.06667	.07500	.13333	.06667	.13333	.06667	.13333	.06000	.15085
.2	0	0	.03333	.13333	.06667	.13333	.06667	.13333	.06000	.15085
.3	0	0	-.00833	.06667	.07500	.13333	.06667	.13333	.06000	.15085
.4	0	0	0	0	.03333	.13333	.06667	.13333	.06000	.15085
.5	0	0	0	0	-.00833	.06667	.07500	.13333	.06000	.15085
.6	0	0	0	0	0	0	.03333	.13333	.06000	.15085
.7	0	0	0	0	0	0	-.00833	.06667	.06833	.15085
.8	0	0	0	0	0	0	0	0	.02667	.15085
.9	0	0	0	0	0	0	0	0	-.01886	.09333

TABLE II.—VALUES OF THE INTEGRATING MATRIX  $[K_2]$ 

## (a) Six-Point Solution

$\eta/\epsilon_A$	0	.2	.4	.6	.8	.9
0	0	0.05333	0.05333	0.16000	0.07314	0.13792
.2	-.00167	.01000	.02500	.10667	.05448	.10775
.4	0	0	0	.05333	.03581	.07758
.6	0	0	-.00167	.01000	.01548	.04741
.8	0	0	0	0	-.00152	.01724
.9	0	0	0	0	-.00108	.00419

## (b) Ten-Point Solution

$\eta/\epsilon_A$	0	.1	.2	.3	.4	.5	.6	.7	.8	.9
0	0	0.013333	0.013333	0.040000	0.026667	0.066667	0.040000	0.093333	0.046476	0.137920
.1	-.000417	.002500	.006251	.026667	.020000	.053333	.033333	.080000	.040476	.122835
.2	0	0	0	.013333	.013333	.040000	.026667	.066667	.034477	.107750
.3	0	0	-.000417	.002500	.006251	.026667	.020000	.053333	.028476	.092665
.4	0	0	0	0	0	.013333	.013333	.040000	.022476	.077580
.5	0	0	0	0	-.000417	.002500	.006251	.026667	.016477	.062495
.6	0	0	0	0	0	0	0	.013333	.010476	.047410
.7	0	0	0	0	0	0	-.000417	.002500	.004060	.032325
.8	0	0	0	0	0	0	0	0	-.001523	.017240
.9	0	0	0	0	0	0	0	0	-.001077	.004190

TABLE III.— VALUES OF THE INTEGRATING MATRIX  $[K_3]$ 

## (a) Six-Point Solution

$\eta/s_\Delta$	0	.2	.4	.6	.8	.9
0	0	0	0	0	0	0
.2	.08333	.13333	-.01667	0	0	0
.4	.06667	.26667	.06667	0	0	0
.6	.06667	.26667	.15000	.13333	-.01667	0
.8	.06667	.26667	.13333	.26667	.06667	0
.9	.06667	.26667	.13333	.26667	.10833	.06667

## (b) Ten-Point Solution

$\eta/s_\Delta$	0	.1	.2	.3	.4	.5	.6	.7	.8	.9
0	0	0	0	0	0	0	0	0	0	0
.1	.04167	.06667	-.00833	0	0	0	0	0	0	0
.2	.03333	.13333	.03333	0	0	0	0	0	0	0
.3	.03333	.13333	.07500	.06667	-.00833	0	0	0	0	0
.4	.03333	.13333	.06667	.13333	.03333	0	0	0	0	0
.5	.03333	.13333	.06667	.13333	.07500	.06667	-.00833	0	0	0
.6	.03333	.13333	.06667	.13333	.06667	.13333	.03333	0	0	0
.7	.03333	.13333	.06667	.13333	.06667	.13333	.07500	.06667	-.00833	0
.8	.03333	.13333	.06667	.13333	.06667	.13333	.06667	.13333	.03333	0
.9	.03333	.13333	.06667	.13333	.06667	.13333	.06667	.13333	.07500	.06667

TABLE IV.— VALUES OF THE LOAD-CONVERSION MATRIX  $[K_6]$ 

## (a) Six-Point Solution

$\eta/s_\Delta$	0	.2	.4	.6	.8	.9
0.2	0.08333	0.13333	-0.01667	0	0	0
.4	-0.01667	.13333	.08333	0	0	0
.6	0	0	.08333	.13333	-0.01667	0
.8	0	0	-0.01667	.13333	.08333	0
.9	0	0	0	0	.04553	.05752
1.0	0	0	0	0	-0.01886	.09333

## (b) Ten-Point Solution

$\eta/s_\Delta$	0	.1	.2	.3	.4	.5	.6	.7	.8	.9
0.1	0.04166	0.06667	-0.00833	0	0	0	0	0	0	0
.2	-0.00833	.06667	.04167	0	0	0	0	0	0	0
.3	0	0	.04166	.06667	-0.00833	0	0	0	0	0
.4	0	0	-0.00833	.06667	.04167	0	0	0	0	0
.5	0	0	0	0	.04166	.06667	-0.00833	0	0	0
.6	0	0	0	0	-0.00833	.06667	.04167	0	0	0
.7	0	0	0	0	0	0	.04166	.06667	-0.00833	0
.8	0	0	0	0	0	0	-0.00833	.06667	.04167	0
.9	0	0	0	0	0	0	0	0	.04166	0
1.0	0	0	0	0	0	0	0	0	-0.00833	.09333

TABLE V.— VALUES OF THE LOAD-CONVERSION MATRIX  $[K_7]$ 

## (a) Six-Point Solution

$\eta/s_A$	0	.2	.4	.6	.8	.9
0.2	0.01667	0.16667	0.01667	0	0	0
.4	-.00833	.05000	.11667	.05000	-.00833	0
.6	0	0	.01667	.16667	.01667	0
.8	0	0	-.00833	.05000	.08946	.02035
.9	0	0	0	0	.00631	.08860
1.0	0	0	0	0	-.01077	.04190

## (b) Ten-Point Solution

$\eta/s_A$	0	.1	.2	.3	.4	.5	.6	.7	.8	.9
0.1	0.00833	0.08333	0.00831	0	0	0	0	0	0	0
.2	-.00417	.02500	.05834	.02500	-.00417	0	0	0	0	0
.3	0	0	.00833	.08333	.00833	0	0	0	0	0
.4	0	0	-.00417	.02500	.05834	.02500	-.00417	0	0	0
.5	0	0	0	0	.00833	.08333	.00833	0	0	0
.6	0	0	0	0	-.00417	.02500	.05834	.02500	-.00417	0
.7	0	0	0	0	0	0	.00833	.08333	.00835	0
.8	0	0	0	0	0	0	-.00417	.02500	.06029	.02035
.9	0	0	0	0	0	0	0	0	.00631	.08860
1.0	0	0	0	0	0	0	0	0	-.01077	.04190



TABLE VI.— FORM FOR COMPUTATION OF AEROELASTIC MATRIX

## (a) Wing Parameters

$A =$	$S =$	$w =$	$Q_{\phi T} =$
$\Lambda =$	$b =$	$\bar{c} = \frac{S}{b} =$	$Q_{\phi M} =$
$\tan \Lambda =$	$s_{\Lambda} =$	$ac_{sub}$	$Q_{\Gamma T} =$
$\cos \Lambda =$	$s_w = s_{\Lambda} \cos \Lambda =$	$ac_{spr}$	$Q_{\Gamma M} =$

$\eta/s_{\Lambda}$	$\eta$	$c$	$e$	$e_{lsub}$	$e_{lspr}$	$GJ$	$EI$
0							
.2							
.4							
.6							
.8							
.9							

$\left[\frac{c}{\bar{c}_r}\right]$						
$\eta/s_{\Lambda}$	0	.2	.4	.6	.8	.9
0	1.000	0	0	0	0	0
.2	0		0	0	0	0
.4	0	0		0	0	0
.6	0	0	0		0	0
.8	0	0	0	0		0
.9	0	0	0	0	0	

$[I_o]$						
$\eta/s_{\Lambda}$	0	.2	.4	.6	.8	.9
0	0	0	0	0	0	0
.2	1	0	0	0	0	0
.4	1	0	0	0	0	0
.6	1	0	0	0	0	0
.8	1	0	0	0	0	0
.9	1	0	0	0	0	0

$\left[\frac{(GJ)_r}{GJ}\right]$						
$\eta/s_{\Lambda}$	0	.2	.4	.6	.8	.9
0	1.000	0	0	0	0	0
.2	0		0	0	0	0
.4	0	0		0	0	0
.6	0	0	0		0	0
.8	0	0	0	0		0
.9	0	0	0	0	0	

$\left[\frac{(EI)_r}{EI}\right]$						
$\eta/s_{\Lambda}$	0	.2	.4	.6	.8	.9
0	1.000	0	0	0	0	0
.2	0		0	0	0	0
.4	0	0		0	0	0
.6	0	0	0		0	0
.8	0	0	0	0		0
.9	0	0	0	0	0	

$\left[\frac{e_l}{e_{lr}} \left(\frac{c}{\bar{c}_r}\right)^2\right]_{sub}$						
$\eta/s_{\Lambda}$	0	.2	.4	.6	.8	.9
0	1.000	0	0	0	0	0
.2	0		0	0	0	0
.4	0	0		0	0	0
.6	0	0	0		0	0
.8	0	0	0	0		0
.9	0	0	0	0	0	

$\left[\frac{e_l}{e_{lr}} \left(\frac{c}{\bar{c}_r}\right)^2\right]_{spr}$						
$\eta/s_{\Lambda}$	0	.2	.4	.6	.8	.9
0	1.000	0	0	0	0	0
.2	0		0	0	0	0
.4	0	0		0	0	0
.6	0	0	0		0	0
.8	0	0	0	0		0
.9	0	0	0	0	0	

TABLE VI.— FORM FOR COMPUTATION OF AEROELASTIC MATRIX — Continued

## (b) Computing Instructions

①	$[K_3] \left[ \frac{(GJ)_F}{GJ} \right]$					
$\eta/s_A$	0	.2	.4	.6	.8	.9
0	0	0	0	0	0	0
.2	.08333			0	0	0
.4	.06667			0	0	0
.6	.06667					0
.8	.06667					0
.9	.06667					

②	$[K_3] \left[ \frac{(EI)_F}{EI} \right]$					
$\eta/s_A$	0	.2	.4	.6	.8	.9
0	0	0	0	0	0	0
.2	.08333			0	0	0
.4	.06667			0	0	0
.6	.06667					0
.8	.06667					0
.9	.06667					

③	$\frac{(GJ)_F}{(EI)_F} (\tan^2 \Lambda) [2]$					
$\eta/s_A$	0	.2	.4	.6	.8	.9
0	0	0	0	0	0	0
.2				0	0	0
.4				0	0	0
.6						0
.8						0
.9						
$\frac{(GJ)_F}{(EI)_F} \tan^2 \Lambda =$						

④	$\frac{v}{E_w} (Q_{\alpha_T} - Q_{\alpha_M} \tan \Lambda) [I_0]$					
$\eta/s_A$	0	.2	.4	.6	.8	.9
0	0	0	0	0	0	0
.2		0	0	0	0	0
.4		0	0	0	0	0
.6		0	0	0	0	0
.8		0	0	0	0	0
.9		0	0	0	0	0
$\frac{v}{E_w} (Q_{\alpha_T} - Q_{\alpha_M} \tan \Lambda) =$						

⑤	[1] + [3] + [4]					
$\eta/s_A$	0	.2	.4	.6	.8	.9
0	0	0	0	0	0	0
.2				0	0	0
.4				0	0	0
.6						0
.8						0
.9						

⑥	$[K_1] \left[ \frac{e_1}{e_{1r}} \left( \frac{c}{c_r} \right)^2 \right]_{sub}$					
$\eta/s_A$	0	.2	.4	.6	.8	.9
0	0.06667					
.2	-.01667					
.4	0	0				
.6	0	0				
.8	0	0	0	0		
.9	0	0	0	0		

⑦	[5] [6]					
$\eta/s_A$	0	.2	.4	.6	.8	.9
0	0	0	0	0	0	0
.2						
.4						
.6						
.8						
.9						

⑧	$\frac{d}{a} [2]$					
$\eta/s_A$	0	.2	.4	.6	.8	.9
0	0	0	0	0	0	0
.2				0	0	0
.4				0	0	0
.6						0
.8						0
.9						
$\frac{d}{a} = \frac{(GJ)_F}{(EI)_F} \frac{s_A}{e_{1r} c_r \cos \Lambda} \tan \Lambda =$						

⑨	$\frac{v}{E_w} \frac{s_A}{e_{1r} c_r \cos \Lambda} Q_{\alpha_M} [I_0]$					
$\eta/s_A$	0	.2	.4	.6	.8	.9
0	0	0	0	0	0	0
.2		0	0	0	0	0
.4		0	0	0	0	0
.6		0	0	0	0	0
.8		0	0	0	0	0
.9		0	0	0	0	0
$\frac{v}{E_w} \frac{s_A}{e_{1r} c_r \cos \Lambda} Q_{\alpha_M} =$						

⑩	[8] - [9]					
$\eta/s_A$	0	.2	.4	.6	.8	.9
0	0	0	0	0	0	0
.2				0	0	0
.4				0	0	0
.6						0
.8						0
.9						

TABLE VI.-- FORM FOR COMPUTATION OF AEROELASTIC MATRIX - Concluded

(b) Computing Instructions - Concluded

## Subsonic Case

(11)	$[K_2] \left[ \frac{c}{c_r} \right]$					
$\eta/s_\Lambda$	0	.2	.4	.6	.8	.9
0	0					
.2	-.00167					
.4	0	0	0			
.6	0	0				
.8	0	0	0	0		
.9	0	0	0	0		

(12)	$[10] [11]$					
$\eta/s_\Lambda$	0	.2	.4	.6	.8	.9
0	0	0	0	0	0	0
.2						
.4						
.6						
.8						
.9						

(13)	$[A] = [7] - [12]$					
$\eta/s_\Lambda$	0	.2	.4	.6	.8	.9
0	0	0	0	0	0	0
.2						
.4						
.6						
.8						
.9						

## Supersonic Case

(6a)	$[K_1] \left[ \frac{e_1}{e_{1r}} \left( \frac{c}{c_r} \right)^2 \right]_{spr}$					
$\eta/s_\Lambda$	0	.2	.4	.6	.8	.9
0	0.06667					
.2	-.01667					
.4	0	0				
.6	0	0				
.8	0	0	0	0		
.9	0	0	0	0		

(7a)	$[5] [6a]$					
$\eta/s_\Lambda$	0	.2	.4	.6	.8	.9
0	0	0	0	0	0	0
.2						
.4						
.6						
.8						
.9						

(12a)	$\frac{(e_{1r})_{sub}}{(e_{1r})_{spr}} [12]$					
$\eta/s_\Lambda$	0	.2	.4	.6	.8	.9
0	0	0	0	0	0	0
.2						
.4						
.6						
.8						
.9						
$\frac{(e_{1r})_{sub}}{(e_{1r})_{spr}} = \underline{\hspace{2cm}}$						

(13a)	$[A] = [7a] - [12a]$					
$\eta/s_\Lambda$	0	.2	.4	.6	.8	.9
0	0	0	0	0	0	0
.2						
.4						
.6						
.8						
.9						

TABLE VII.-- FORM FOR SOLUTION OF AEROELASTIC EQUATION

(b) Aerodynamic Loading

(a) Divergence

$$\frac{a}{a_D} = \quad a = \quad$$

$[A]$						
$\eta/\epsilon_A$	0	.2	.4	.6	.8	.9
0	0	0	0	0	0	0
.2						
.4						
.6						
.8						
.9						

$[I] - a[A]$						
$\eta/\epsilon_A$	0	.2	.4	.6	.8	.9
0	1.0000	0	0	0	0	0
.2						
.4						
.6						
.8						
.9						

$\{a_g\}_a$	$\{a_g\}_p$	$\{a_g\}_-$
1		
1		
1		
1		
1		
1		

Auxiliary matrices

$\{a_g\}$						
	(1)	(2)	(3)	(4)	(5)	(6)
0	0	0	0	0	0	0
.2	.3000					
.4	.5000					
.6	.7000					
.8	.9000					
.9	1.0000	1.0000	1.0000	1.0000	1.0000	1.0000

0	1.0000	0	0	0	0	0
.2						
.4						
.6						
.8						
.9						

1.0000		

Final matrices

$[A]\{a_g\}$						
	(1)	(2)	(3)	(4)	(5)	(6)
0	0	0	0	0	0	0
.2						
.4						
.6						
.8						
.9						

$[K_1]_1 [c/c_T]$						
①						

$[K_2]_1 [c/c_T]$						
②						

$\left\{\frac{m_0}{m_{e1}} \bar{\alpha}\right\}_a$	$\left\{\frac{m_0}{m_{e1}} \bar{\alpha}\right\}_p$	$\left\{\frac{m_0}{m_{e1}} \bar{\alpha}\right\}_-$

$\left\{\frac{m_0}{m_{e1}} \bar{\alpha}\right\}_a =$	$\left\{\frac{m_0}{m_{e1}} \bar{\alpha}\right\}_p =$	$\left\{\frac{m_0}{m_{e1}} \bar{\alpha}\right\}_- =$
$\left\{\frac{m_0}{m_{e1}} \bar{\alpha}\right\}_a =$	$\left\{\frac{m_0}{m_{e1}} \bar{\alpha}\right\}_p =$	$\left\{\frac{m_0}{m_{e1}} \bar{\alpha}\right\}_- =$

$$a_D =$$

$C_{L_w} =$	$C_{M_w} =$	$C_{Z_w} =$	$\frac{\bar{y}}{s_w} =$
-------------	-------------	-------------	-------------------------

NACA

TABLE VIII.-- PARAMETERS OF EXAMPLE WING

$A = 4$	$S = 37498$	$w = 22.4$	$Q_{\Psi T} = 0$
$\Lambda = 37.5^\circ$	$b = 387.4$	$\bar{c} = \frac{S}{b} = 96.8$	$Q_{\Psi M} = 0.40$
$\tan \Lambda = 0.7673$	$s_\Lambda = 218.9$	$ac_{sub} = 0.25$	$Q_{\Gamma T} = 1.60$
$\cos \Lambda = 0.7934$	$s_w = s_\Lambda \cos \Lambda = 173.7$	$ac_{spr} = 0.425$	$Q_{\Gamma M} = -0.25$

$\eta/s_\Lambda$	$\eta$	$c$	$e$	$e_{1sub}$	$e_{1spr}$	$GJ$	$EI$
0	0	122.5	0.4522	0.202	0.0272	$6.56 \times 10^9$	$7.02 \times 10^9$
.2	43.8	110.8	.4493	.199	.0243	5.79	6.28
.4	87.6	99.3	.4469	.197	.0219	3.13	3.65
.6	131.3	87.7	.4444	.194	.0194	1.49	1.89
.8	175.1	76.2	.4420	.192	.0170	.68	.94
.9	197.0	70.3	.4407	.191	.0157	.42	.64

$\left[\frac{c}{c_r}\right]$						
$\eta/s_\Lambda$	0	.2	.4	.6	.8	.9
0	1.000	0	0	0	0	0
.2	0	.905	0	0	0	0
.4	0	0	.811	0	0	0
.6	0	0	0	.716	0	0
.8	0	0	0	0	.622	0
.9	0	0	0	0	0	.574

$[I_o]$						
$\eta/s_\Lambda$	0	.2	.4	.6	.8	.9
0	0	0	0	0	0	0
.2	1	0	0	0	0	0
.4	1	0	0	0	0	0
.6	1	0	0	0	0	0
.8	1	0	0	0	0	0
.9	1	0	0	0	0	0

$\left[\frac{(GJ)_r}{GJ}\right]$						
$\eta/s_\Lambda$	0	.2	.4	.6	.8	.9
0	1.000	0	0	0	0	0
.2	0	1.13	0	0	0	0
.4	0	0	2.10	0	0	0
.6	0	0	0	4.40	0	0
.8	0	0	0	0	9.64	0
.9	0	0	0	0	0	15.61

$\left[\frac{(EI)_r}{EI}\right]$						
$\eta/s_\Lambda$	0	.2	.4	.6	.8	.9
0	1.00	0	0	0	0	0
.2	0	1.12	0	0	0	0
.4	0	0	1.92	0	0	0
.6	0	0	0	3.71	0	0
.8	0	0	0	0	7.47	0
.9	0	0	0	0	0	10.96

$\left[\frac{e_1}{e_{1r}} \left(\frac{c}{c_r}\right)^2\right]_{sub}$						
$\eta/s_\Lambda$	0	.2	.4	.6	.8	.9
0	1.000	0	0	0	0	0
.2	0	.806	0	0	0	0
.4	0	0	.642	0	0	0
.6	0	0	0	.492	0	0
.8	0	0	0	0	.368	0
.9	0	0	0	0	0	.312

$\left[\frac{e_1}{e_{1r}} \left(\frac{c}{c_r}\right)^2\right]_{spr}$						
$\eta/s_\Lambda$	0	.2	.4	.6	.8	.9
0	1.000	0	0	0	0	0
.2	0	.732	0	0	0	0
.4	0	0	.530	0	0	0
.6	0	0	0	.366	0	0
.8	0	0	0	0	.242	0
.9	0	0	0	0	0	.190

TABLE IX.—COMPUTATION OF AEROELASTIC MATRIX OF EXAMPLE WING  
(SUBSONIC CASE)

①	$[K_3] \left[ \frac{(GJ)_r}{(EI)_r} \right]$					
$\eta/s_A$	0	.2	.4	.6	.8	.9
0	0	0	0	0	0	0
.2	.08333	.15066	-.03501	0	0	0
.4	.06667	.30134	.14001	0	0	0
.6	.06667	.30134	.31500	.58665	-.16070	0
.8	.06667	.30134	.27999	1.17335	.64270	0
.9	.06667	.30134	.27999	1.17335	1.04430	1.04072

②	$[K_3] \left[ \frac{(EI)_r}{EI} \right]$					
$\eta/s_A$	0	.2	.4	.6	.8	.9
0	0	0	0	0	0	0
.2	.08333	.14933	-.03201	0	0	0
.4	.06667	.29867	.12801	0	0	0
.6	.06667	.29867	.28800	.49465	-.12452	0
.8	.06667	.29867	.25599	.98935	.49802	0
.9	.06667	.29867	.25599	.98935	.80923	.73070

③	$\frac{(GJ)_r}{(EI)_r} (\tan^2 \Lambda) \text{ [2]}$					
$\eta/s_A$	0	.2	.4	.6	.8	.9
0	0	0	0	0	0	0
.2	.04585	.08216	-.01761	0	0	0
.4	.03668	.16433	.07043	0	0	0
.6	.03668	.16433	.15846	.27216	-.06851	0
.8	.03668	.16433	.14085	.54434	.27401	0
.9	.03668	.16433	.14085	.54434	.44524	.40203
$\frac{(GJ)_r}{(EI)_r} \tan^2 \Lambda = 0.5502$						

④	$\frac{V}{s_W} (Q_{WT} - Q_{WM} \tan \Lambda) [I_0]$					
$\eta/s_A$	0	.2	.4	.6	.8	.9
0	0	0	0	0	0	0
.2	-.1629	0	0	0	0	0
.4	-.1629	0	0	0	0	0
.6	-.1629	0	0	0	0	0
.8	-.1629	0	0	0	0	0
.9	-.1629	0	0	0	0	0
$\frac{V}{s_W} (Q_{WT} - Q_{WM} \tan \Lambda) = -0.1629$						

⑤	① + ③ + ④					
$\eta/s_A$	0	.2	.4	.6	.8	.9
0	0	0	0	0	0	0
.2	-.03372	.23282	-.05262	0	0	0
.4	-.05955	.46567	.21044	0	0	0
.6	-.05955	.46567	.47346	.85881	-.22921	0
.8	-.05955	.46567	.42084	1.71769	.91671	0
.9	-.05955	.46567	.42084	1.71769	1.48954	1.44275

⑥	$[K_1] \left[ \frac{e_1}{e_r} \left( \frac{c}{c_r} \right)^2 \right]_{\text{sub}}$					
$\eta/s_A$	0	.2	.4	.6	.8	.9
0	0.06667	0.21494	0.08560	0.13120	0.03435	0.04707
.2	-.01667	.10746	.09630	.13120	.03435	.04707
.4	0	0	.04280	.13120	.03435	.04707
.6	0	0	-.01070	.06560	.04048	.04707
.8	0	0	0	0	.00981	.04707
.9	0	0	0	0	-.00694	.02912

⑦	⑤ [6]					
$\eta/s_A$	0	.2	.4	.6	.8	.9
0	0	0	0	0	0	0
.2	-.00613	.01777	.01728	.01922	.00503	.00689
.4	-.01173	.03724	.04875	.08089	.02118	.02902
.6	-.01173	.03724	.05082	.17174	.06273	.07104
.8	-.01173	.03724	.03938	.22118	.10693	.16293
.9	-.01173	.03724	.03938	.22118	.10254	.23190

⑪	$[K_2] \left[ \frac{e}{e_r} \right]$					
$\eta/s_A$	0	.2	.4	.6	.8	.9
0	0	0.04826	0.04325	0.11456	0.04549	0.07917
.2	-.00167	.00905	.02028	.07638	.03389	.06185
.4	0	0	0	.03818	.02227	.04453
.6	0	0	-.00135	.00716	.00963	.02721
.8	0	0	0	0	-.00095	.00990
.9	0	0	0	0	-.00067	.00241

⑫	⑩ [11]					
$\eta/s_A$	0	.2	.4	.6	.8	.9
0	0	0	0	0	0	0
.2	-.00199	.01106	.02444	.08202	.03500	.06286
.4	-.00399	.01543	.04289	.20681	.09790	.18314
.6	-.00399	.01543	.03755	.28397	.16542	.33786
.8	-.00399	.01543	.03221	.30252	.19308	.48336
.9	-.00399	.01543	.03221	.30252	.18680	.52208

⑬	[A] = [7] - [12]					
$\eta/s_A$	0	.2	.4	.6	.8	.9
0	0	0	0	0	0	0
.2	-.00414	.00671	-.00716	-.06280	-.02997	-.05597
.4	-.00774	.02181	.00586	-.12592	-.07672	-.15412
.6	-.00774	.02181	.01327	-.11223	-.10269	-.26682
.8	-.00774	.02181	.00717	-.08134	-.08615	-.32043
.9	-.00774	.02181	.00717	-.08134	-.08426	-.29018

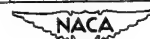


TABLE I.— SOLUTION OF AEROELASTIC EQUATION FOR EXAMPLE WING (SUBSONIC CASE)

(b) Aerodynamic Loading

(a) Divergence

$$\frac{a}{ap} = -0.25 \quad a = 0.552$$

[A]						
$\eta/\epsilon_A$	0	.2	.4	.6	.8	.9
0	0	0	0	0	0	0
.2	-.0041	.0067	-.0072	-.0628	-.0300	-.0560
.4	-.0077	.0218	.0059	-.1259	-.0767	-.1541
.6	-.0077	.0218	.0133	-.1122	-.1027	-.2668
.8	-.0077	.0218	.0072	-.0813	-.0862	-.3204
.9	-.0077	.0218	.0072	-.0813	-.0843	-.2902

[I] - a[A]						
$\eta/\epsilon_A$	0	.2	.4	.6	.8	.9
0	1.0000	0	0	0	0	0
.2	.0023	.9963	.0040	.0347	.0165	.0309
.4	.0043	-.0120	.9968	.0695	.0424	.0851
.6	.0043	-.0120	-.0073	1.0620	.0567	.1473
.8	.0043	-.0120	-.0040	.0449	1.0476	.1769
.9	.0043	-.0120	-.0040	.0449	.0465	1.1602

$\{a_s\}_a$	$\{a_s\}_p$	$\{a_s\}_-$
1	0.1033	
1	.2826	
1	.4620	
1	.6413	
1	.8207	
1	.9103	

Auxiliary matrices

$\{a_s\}$						
	(1)	(2)	(3)	(4)	(5)	(6)
0	0	0	0	0	0	0
.2	.3000	.3115	.3449	.3480		
.4	.5000	.7311	.7846	.7876		
.6	.7000	1.0286	1.0526	1.0532		
.8	.9000	1.0775	1.0714	1.0713		
.9	1.0000	1.0000	1.0000	1.0000	1.0000	1.0000

0	1.0000	0	0	0	0	0
.2	.0023	.9963	.0040	.0348	.0166	.0310
.4	.0043	-.0120	.9968	.0702	.0427	.0857
.6	.0043	-.0120	-.0073	1.0629	.0538	.1395
.8	.0043	-.0120	.0039	.0456	1.0455	.1638
.9	.0043	-.0120	.0039	.0456	.0444	1.1473

1.0000	0.1033	
1.0014	.2834	
1.0110	.4665	
.9551	.6094	
.9261	.7630	
.8081	.7439	

Final matrices

[A] $\{a_s\}$						
	(1)	(2)	(3)	(4)	(5)	(6)
0	0	0	0	0	0	0
.2	-.1286	-.1561	-.1576			
.4	-.3018	-.3551	-.3567			
.6	-.4246	-.4764	-.4770			
.8	-.4448	-.4849	-.4852			
.9	-.4128	-.4526	-.4529	-.4529		

$[K_1]_1 \left[ \frac{c}{c_r} \right]$					
①	0.0667	0.2413	0.1081	0.1909	0.0581
				0.0866	

$[K_2]_1 \left[ \frac{c}{c_r} \right]$					
②	0	0.0483	0.0433	0.1146	0.0455
				0.0792	

$\left\{ \frac{m_0}{m_{e1}} \bar{\alpha} \right\}_a$	$\left\{ \frac{m_0}{m_{e1}} \bar{\alpha} \right\}_p$	$\left\{ \frac{m_0}{m_{e1}} \bar{\alpha} \right\}_-$
1.0000	0.1033	
.9320	.2320	
.8518	.3423	
.7996	.4711	
.7937	.6412	
.8081	.7439	

$\left[ \frac{m_0}{m_{e1}} \bar{\alpha} \right]_a = 0.6524$	$\left[ \frac{m_0}{m_{e1}} \bar{\alpha} \right]_p =$	$\left[ \frac{m_0}{m_{e1}} \bar{\alpha} \right]_- =$
$\left[ \frac{m_0}{m_{e1}} \bar{\alpha} \right]_a = 0.2736$	$\left[ \frac{m_0}{m_{e1}} \bar{\alpha} \right]_p = 0.1681$	$\left[ \frac{m_0}{m_{e1}} \bar{\alpha} \right]_- =$

$$a_p = -2.208$$

$C_{L_w} = 0.740 m_{e1}$	$C_{BM_w} = 0.0696 m_{e1}$	$C_{L_w} = 0.0855 m_e$	$\bar{y}_{\bar{v}} = 0.419$
--------------------------	----------------------------	------------------------	-----------------------------

NACA

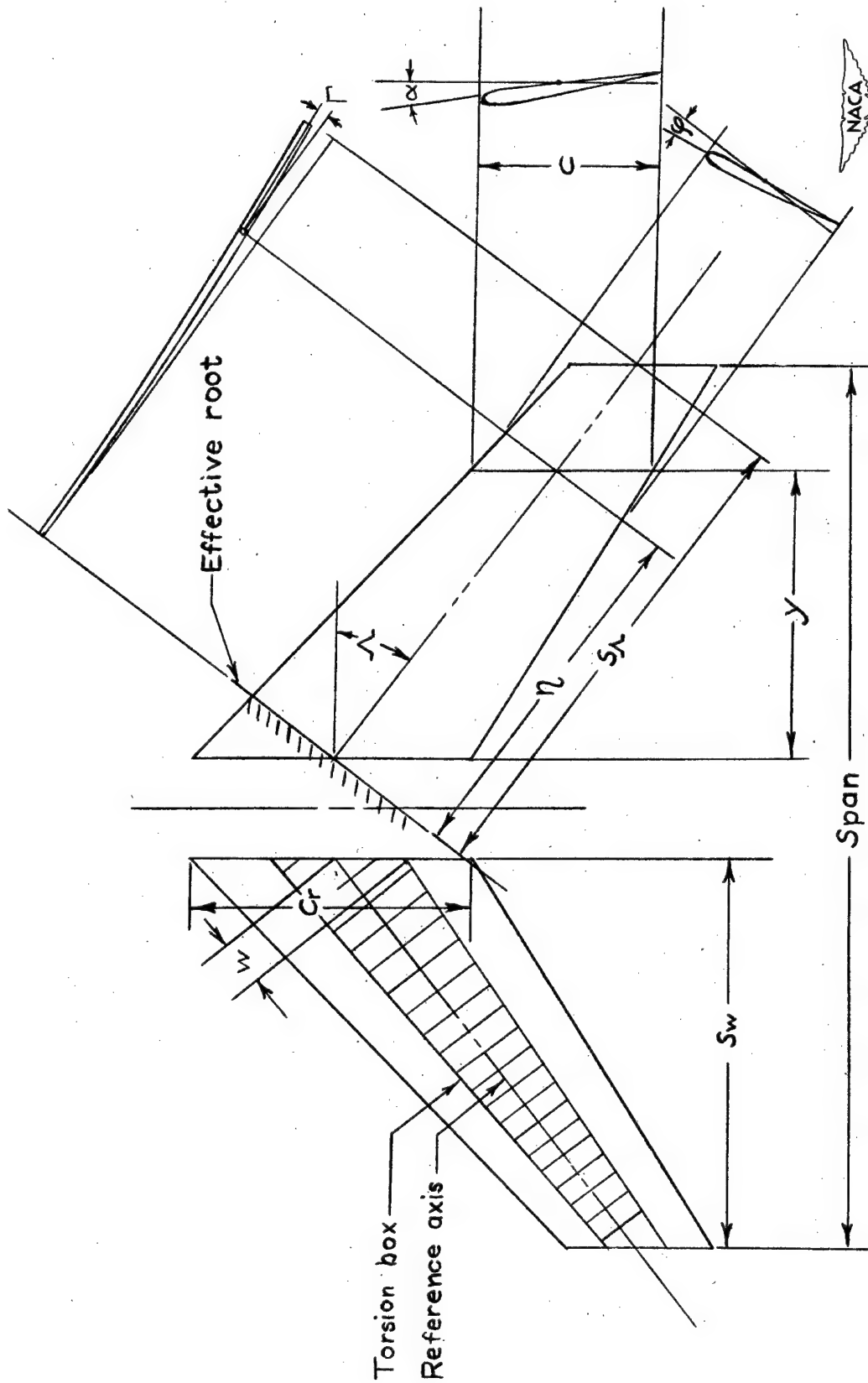
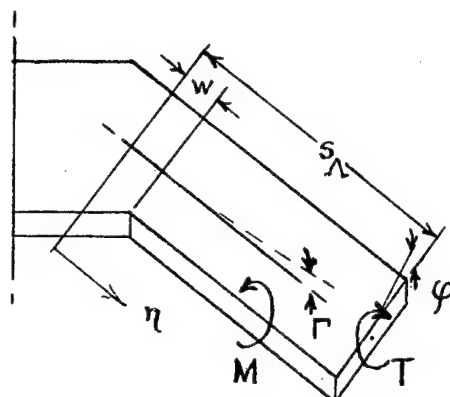


Figure 1.— Definition of geometrical parameters used in the analysis.





$$S_L = 104 \text{ in.}$$

$$w = 15 \text{ in.}$$

$$(GJ)_r = 5.10 \times 10^8 \text{ lb-in.}^2$$

$$(EI)_r = 9.47 \times 10^8 \text{ lb-in.}^2$$

$$T_r = 43,420 \text{ in.-lb}$$

$$M_r = 260,000 \text{ in.-lb}$$

	Rotation	Av. value	Q value
————	$\phi_{rT}$	-0.0002	0.16
-----	$\phi_{rM}$	.0025	.33
- - - - -	$\Gamma_{rT}$	.0010	1.45
- - - - -	$\Gamma_{rM}$	- .0010	- .24

Rotations due to root  
deflections,  $\phi_r$  and  $\Gamma_r$ , radians

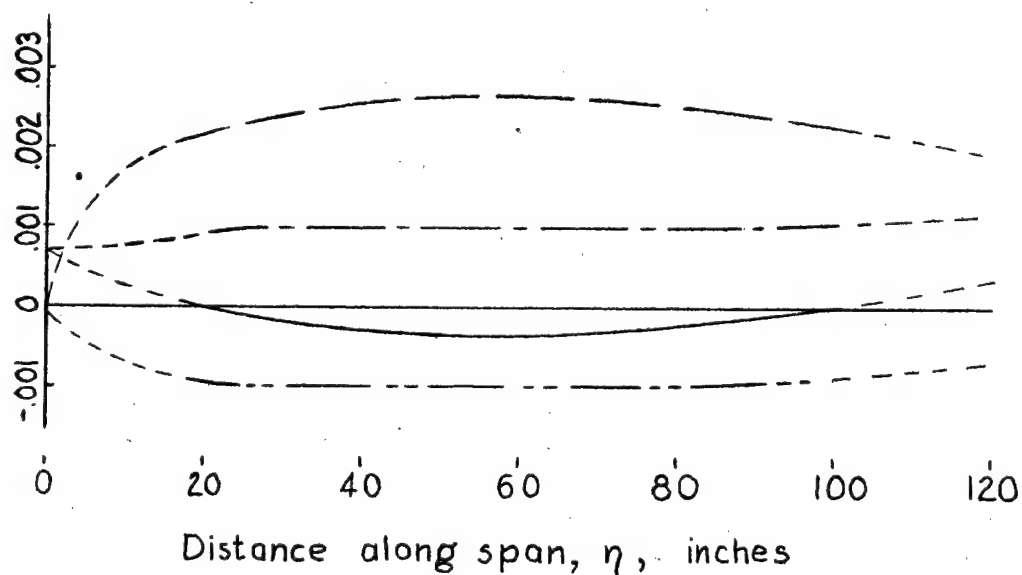


Figure 2.- Rotations of a 45° swept box beam due to root deflections (data from reference 5).

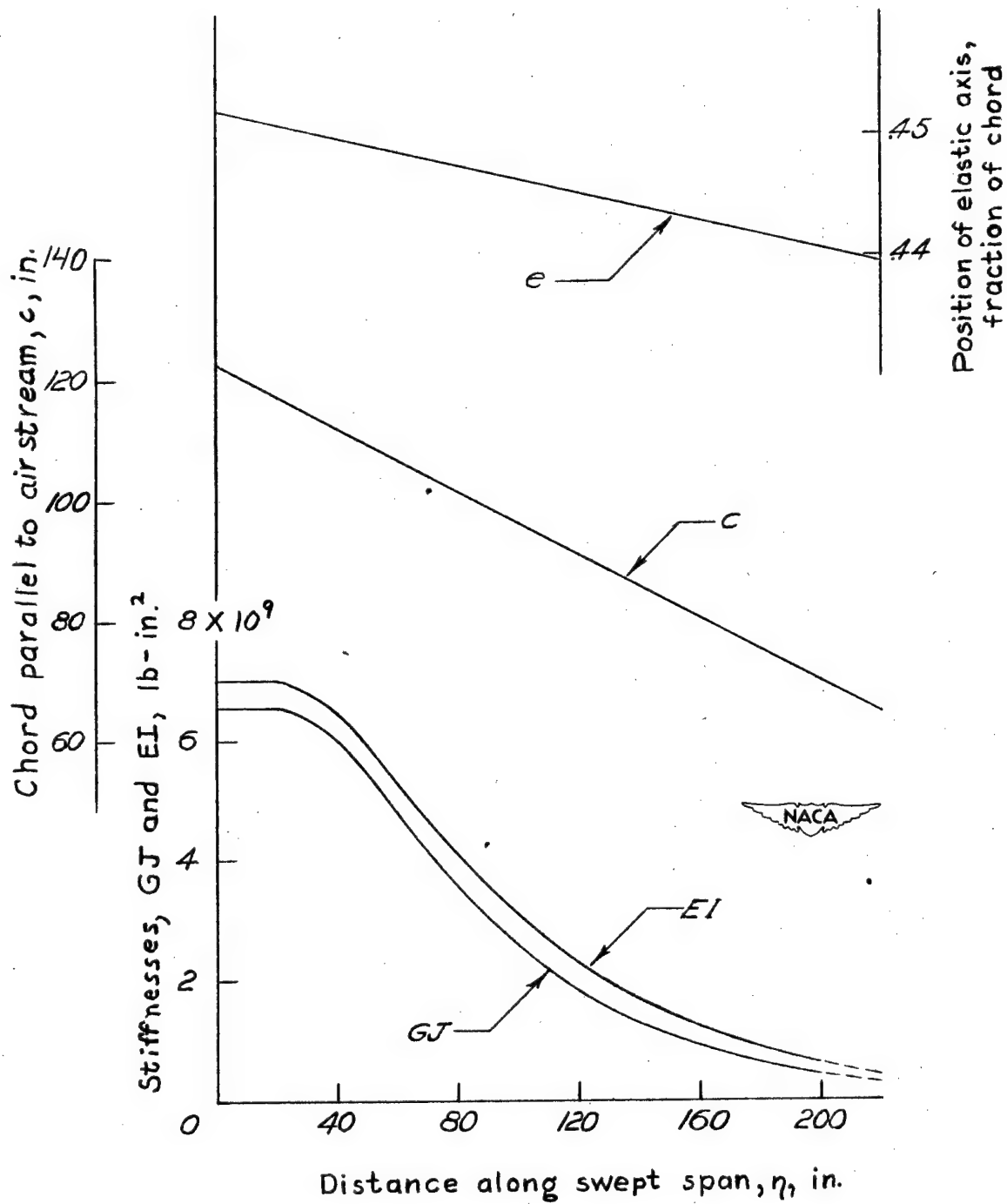


Figure 3.- Parameters of the example wing.

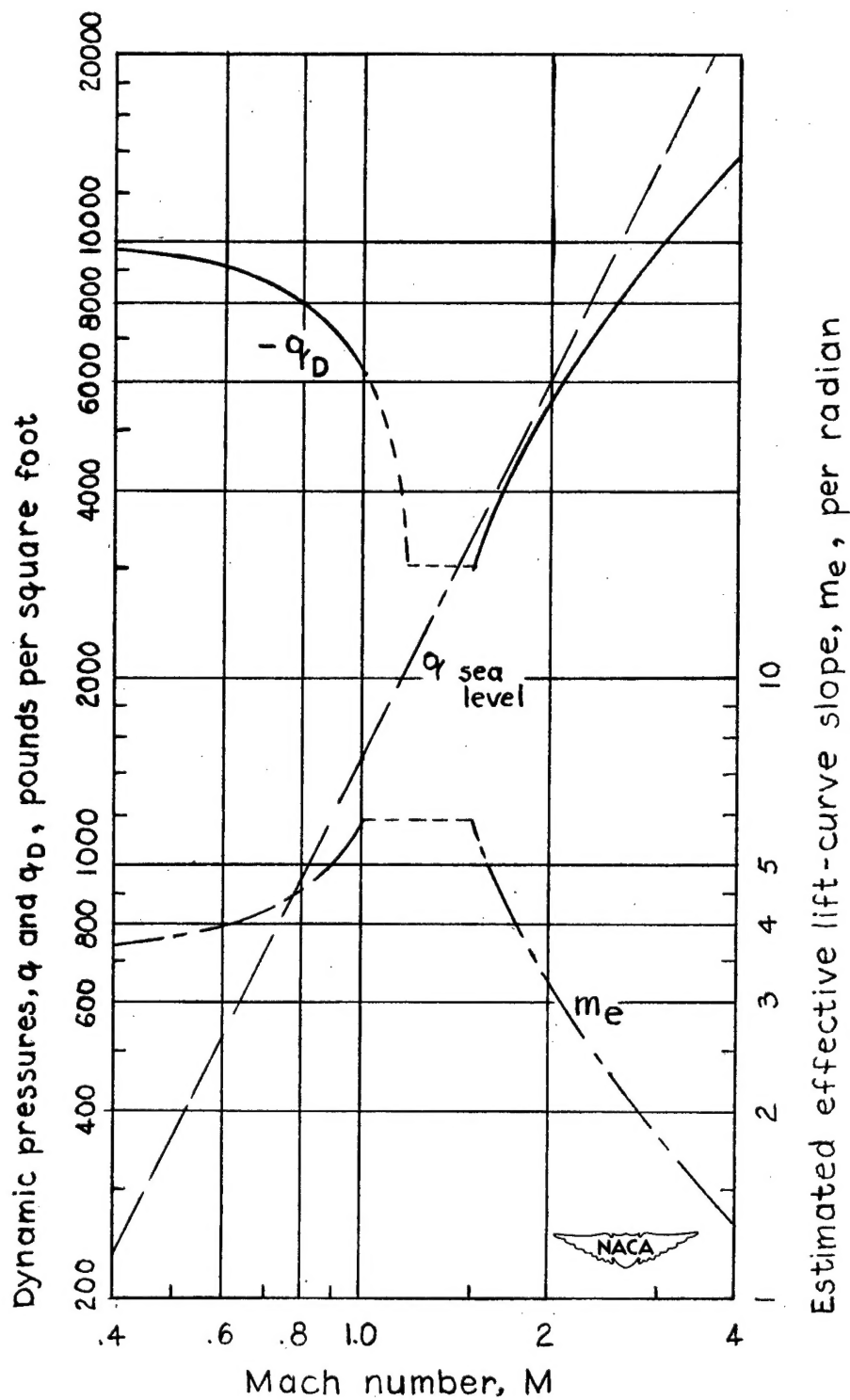
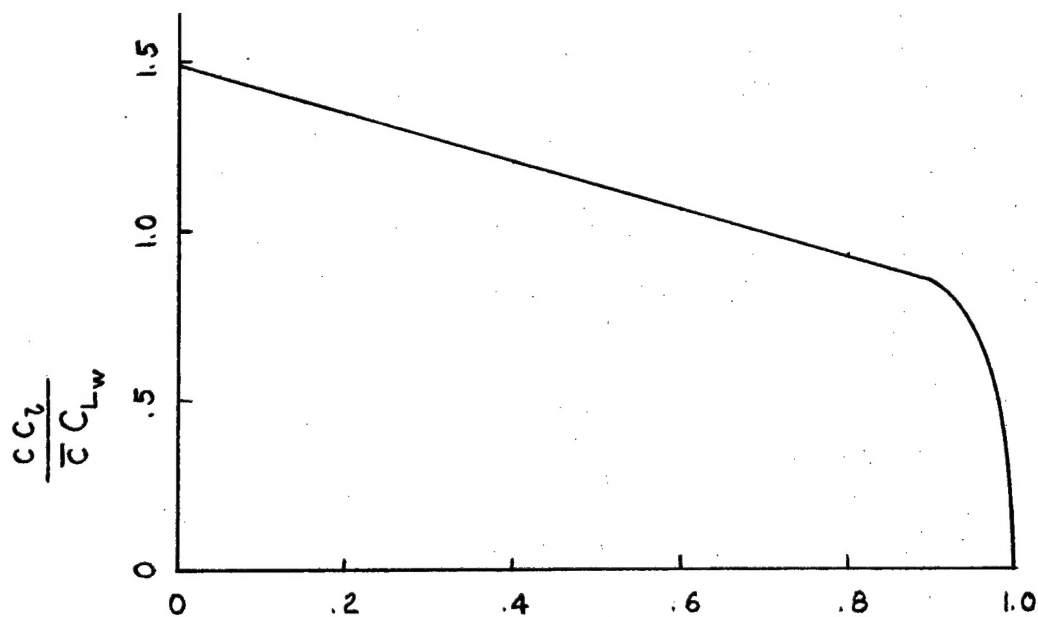
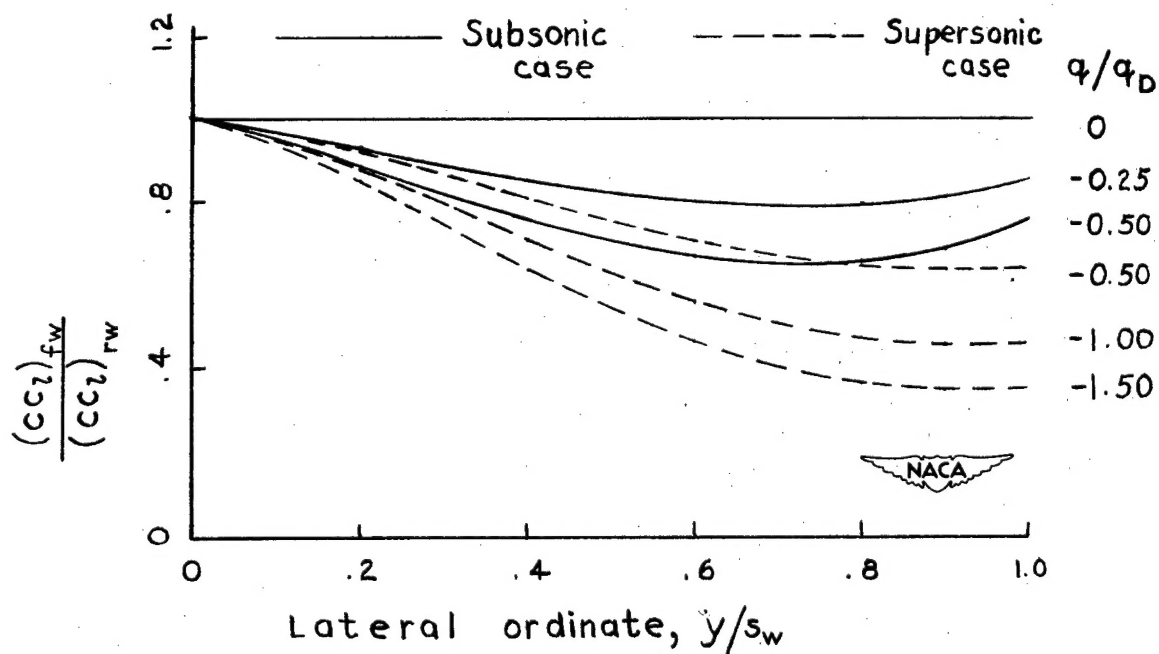


Figure 4.— Effect of Mach number on the divergence dynamic pressure and lift-curve slope of the example wing.



Lateral ordinate,  $y/s_w$   
 (a) Assumed rigid-wing loading.



Lateral ordinate,  $y/s_w$   
 (b) Flexible-wing loading.

Figure 5.- Load distribution of example wing.

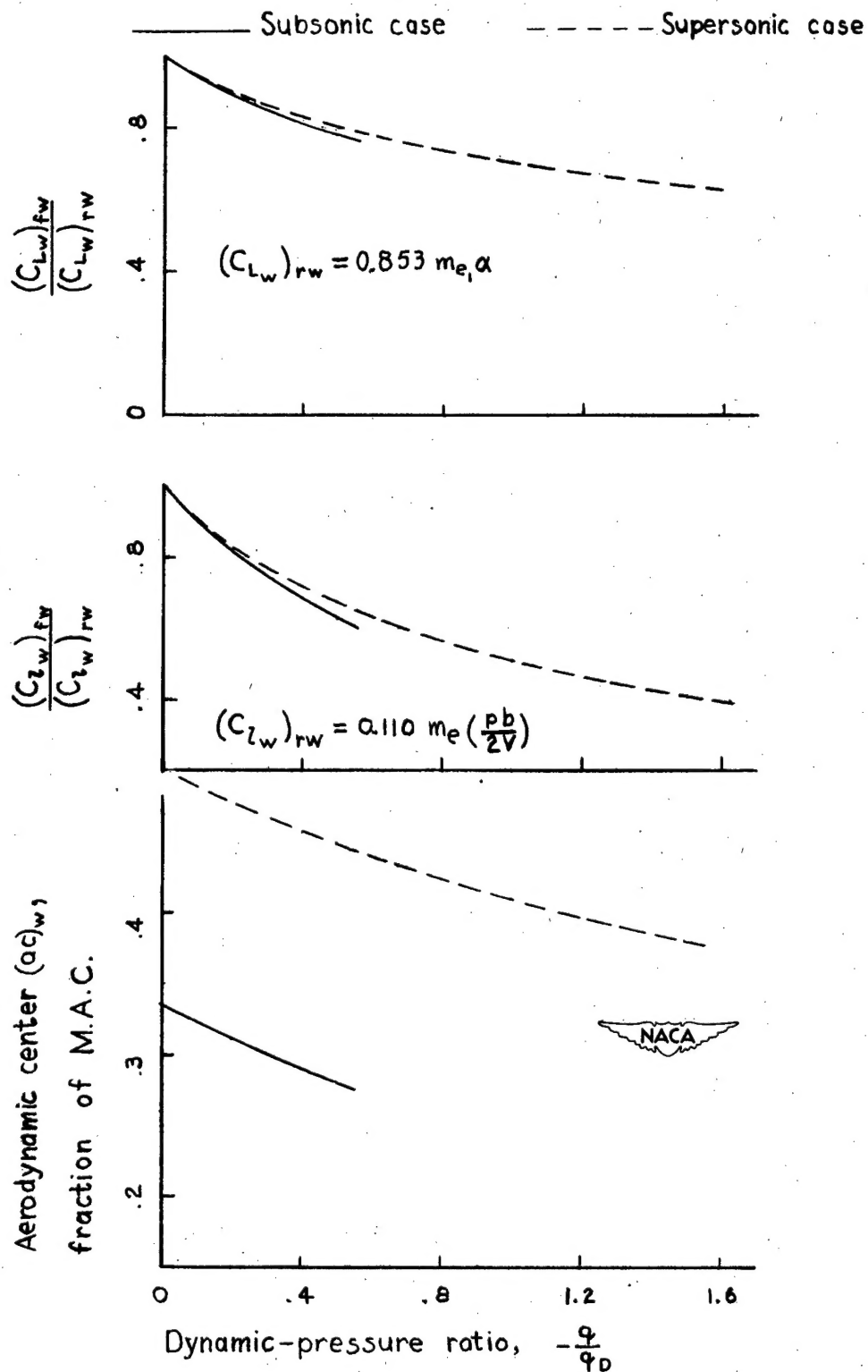


Figure 6.- Lift coefficient, rolling-moment coefficient, and aerodynamic center of example wing.

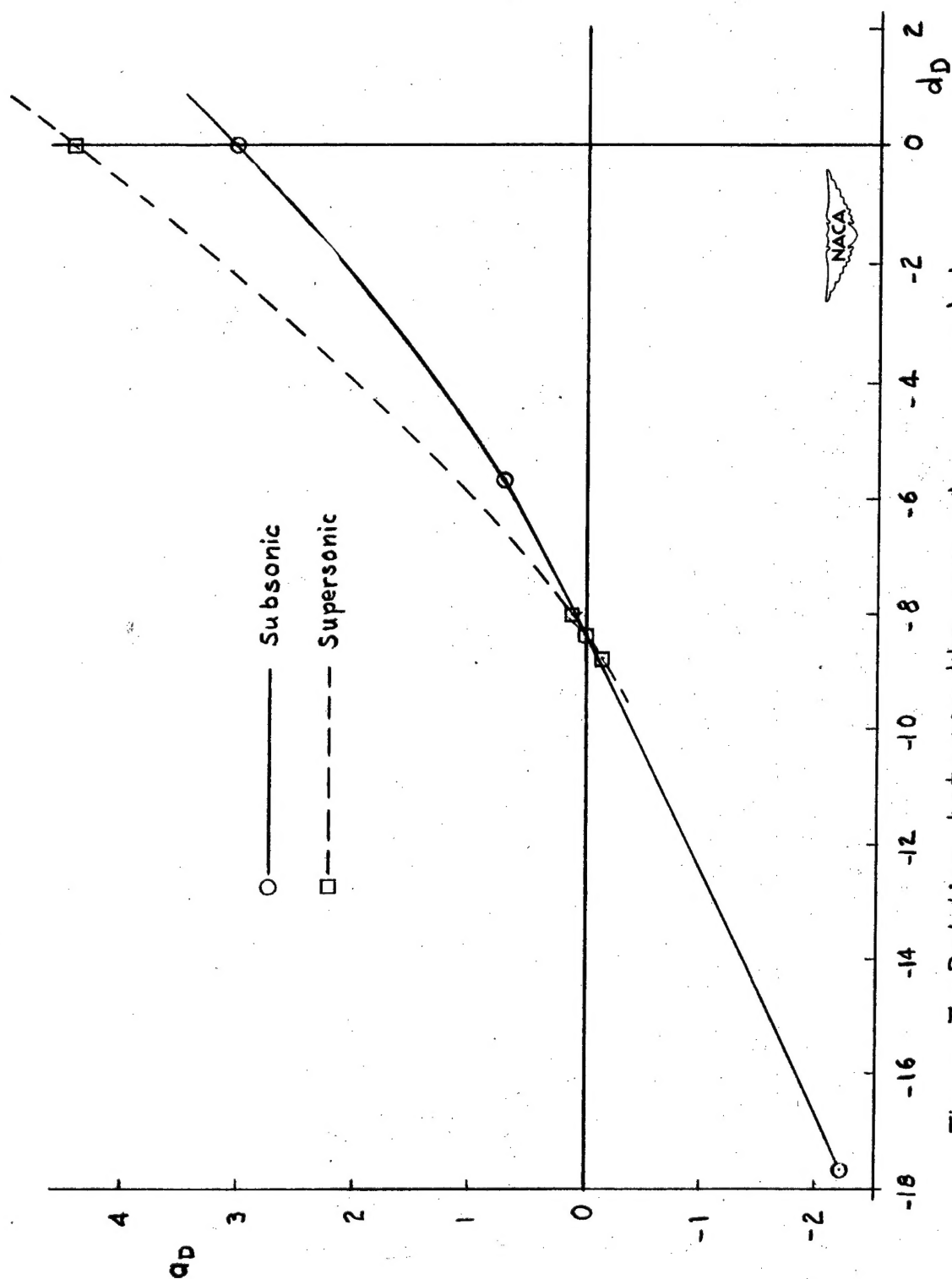


Figure 7.—Relation between the parameters  $q_D$  and  $d_D$ .